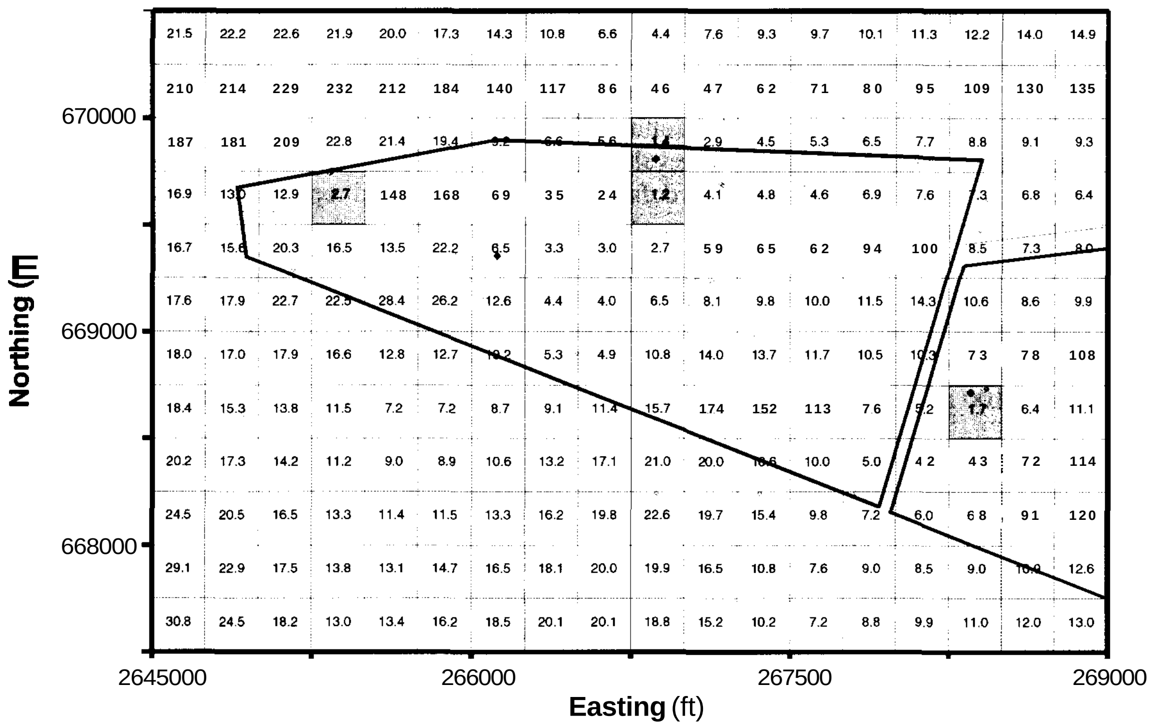

Figure 5-58, The B-C interbed kriged thicknesses with shaded locations where gaps were superimposed.

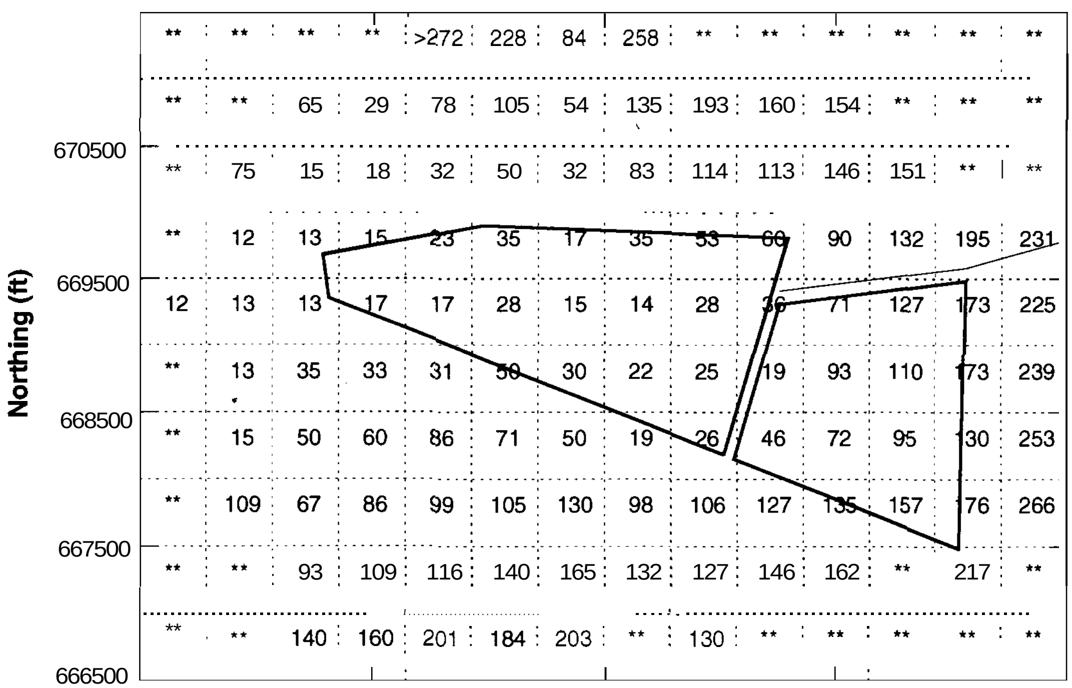

Figure 5-59. Simulated vadose zone water travel times when gaps are included in the B-C interbed.

5.2.6.3 *Plutonium Partition Coefficients.* The plutonium K_d used in the ABRA model and in the IRA model has been carefully examined. The **5,100-mL/g** value selected for the base ABRA simulation was selected as the best site-specific value available. To test the effect of the assigned K_d, a series of simulations was performed in which the plutonium K_d was varied consistently in both the source model and in the vadose zone transport model. The values assigned were **22,320,** and **1,700** mL/g. The **22-mL/g** value was taken from the Track **2** screening default (DOE-ID **1994)** and represents the extreme low end of measured plutonium K_ds. The value is actually an average of four crushed Hanford basalt samples. The second two values are taken from EPA guidance (see Appendix G of EPA **1999),** which was based on work by Glover, Miner, and Polzer **(1976)** and Miner, Evans, and Polzer **(1982).** These latter two values were measured on Polatis-type soil taken from unspecified locations on the INEEL. Polatis soil is described as loess over lava. The selected range represents approximately an order of magnitude of changes from **5,100** mL/g down to **22** mL/g and provides a broad spectrum of possible behavior.

Both **Pu-238** and **Pu-239** were simulated in this sensitivity analysis. The **Pu-240** was not simulated, because results would be similar to **Pu-239.** Comparisons of maximum simulated aquifer concentrations are given in Table **5-18.** The maximum values are for the period beginning in **1952** and ending in calendar year **2001.** Also shown are the maximum observed **Pu-238** and **Pu-239** aquifer concentrations from sampling activities since **1987.** Decreasing K_d for plutonium isotopes increases resulting simulated concentrations, as shown in Table **5-18.** However, even the maximum concentration from the K_d = **22** mL/g simulation is not quite high enough to be detected with normal quarterly sampling conducted by WAG **7** because the instrument detection limit for the analyses is approximately **0.02** pCi/L.

Table **5-18.** Maximum **12-m (39-ft)** depth simulated **Pu-238** and **Pu-239** aquifer concentrations (pCi/L) through calendar year **2001** for the base simulation and plutonium K_d sensitivity simulations.

Contaminant of Potential Concern	Baseline Risk Assessment K_d = 5,100 mL/g	K_d = 1,700 mL/g	K_d = 320 mL/g	&,= 22 mL/g	Range of Observed 3σ Concentrations in the Subsurface Disposal Area Vicinity Wells Since 1987
Pu-238	0	1×10^{-25}	4×10^{-17}	4×10^{-4}	1.8E-02 to 3.7E-01
Pu-239	5×10^{-28}	2×10^{-24}	1×10^{-15}	1×10^{-2}	9.4E-02 to 4.3E+00

Comparison of simulated **Pu-238** and **Pu-239** soil concentrations in the B-C interbed are presented in Figures **5-60** and **5-61** and Table **5-19.** Soil concentrations are determined from simulated aqueous concentrations using the K_d. Contour levels in the figures are for every other order of magnitude beginning at 1×10^{-19} Ci/g up through the maximum value. Two locations with elevated simulated concentrations of **Pu-238** and **Pu-239** are shown in Figures **5-60** and **5-61.** As expected, the simulated soil concentrations increase with decreasing K_ds. The one location that actinides are generally accepted as being detected at depth is for the triad of wells (i.e., Wells **79-2,** DO-2, and TW1) located just northeast of Pit **5.** This well location is included in the region of elevated soil concentrations in the figures. Locations near this well triad have yielded interbed samples that do not indicate similar concentrations. Comparing these sampling results to the simulation results in Figures **5-60** and **5-61** indicates that broad-spread elevated actinide soil concentrations predicted with the lowest plutonium K_d of **22** mL/g are not reasonable. However, the simulation results from the mid-range K_ds of **1,700** and **320** mL/g do not contradict the sampling results because they show maximums lower than observed values.

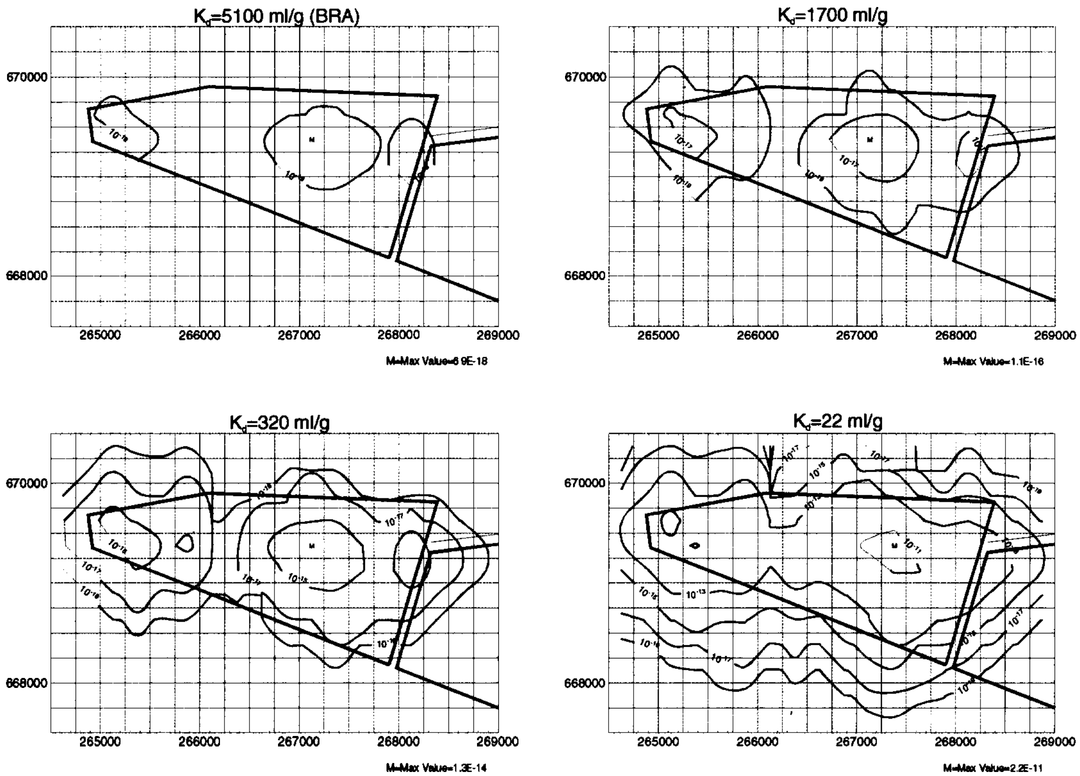

Figure 5-60. Comparison of simulated Pu-238 B-C interbed soil concentrations (Ci/g) for the base simulation to the Pu-238 K_d sensitivity simulations.

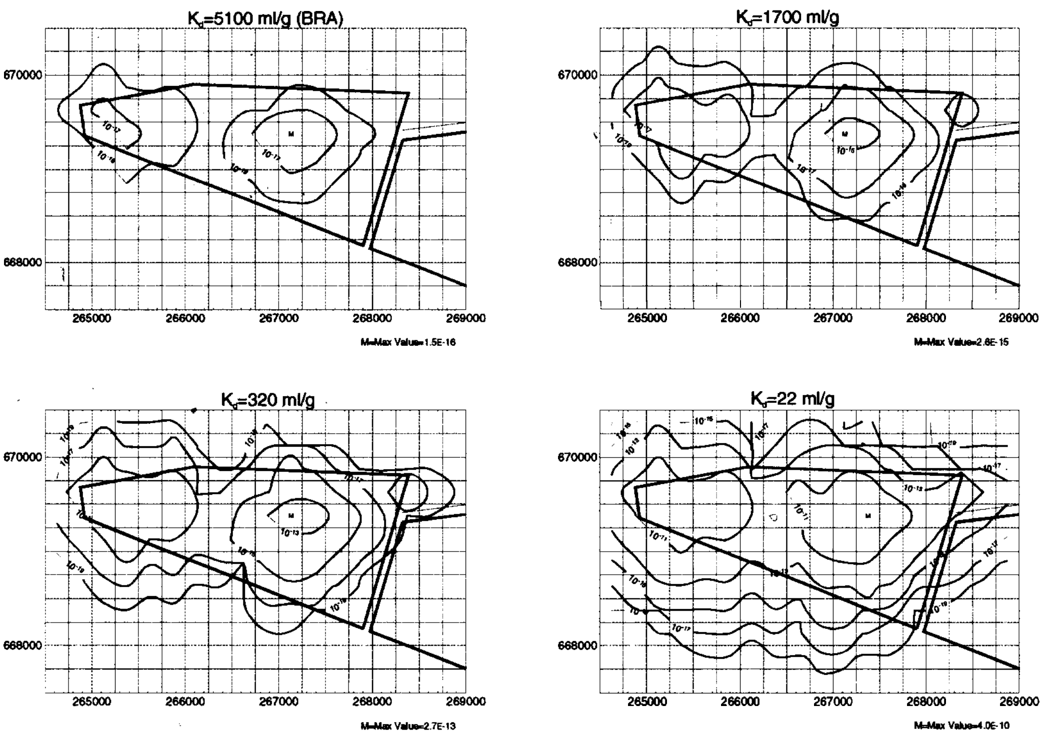

Figure 5-61. Comparison of simulated Pu-239 B-C interbed soil concentrations (Ci/g) for the base simulation and the Pu-238 K_d sensitivity simulations.

Table 5-19. Simulated maximum Pu-238 and Pu-239 B-C interbed soil concentrations (Ci/g) through calendar year 2001 for the base simulation and plutonium K_d sensitivity simulations.

Contaminant of Potential Concern	Base Simulation K_d = 5,100 mL/g	K_d = 1,700 mL/g	K_d = 320 mL/g	K_d = 22 mL/g	Maximum Sampling Results
Pu-238	7×10^{-18}	1×10^{-16}	1×10^{-14}	2×10^{-11}	1×10^{-13}
Pu-239	2×10^{-16}	3×10^{-15}	3×10^{-13}	4×10^{-10}	1×10^{-12}

5.2.6.4 Plutonium Mobile Fractions. Studies on actinide mobility have indicated a potential small mobile fraction of plutonium (Grossman et al. 2001). A series of sensitivity simulations was conducted to test the effect of a small mobile fraction. Both Pu-238 and Pu-239 were simulated in the same manner as for the K_d sensitivity simulations. The source term model was used to release fractions of 1×10^{-6}, 1×10^{-4}, and 1×10^{-2} of the total mass disposed of each year. This range of fractions was very broad and provides a spectrum of possible results. It was necessary to assign a small K_d value of 0.1 mL/g in the sediments and interbeds in the vadose zone model to allow some plutonium to adsorb onto the soil for comparison between predicted and observed soil concentrations in the interbeds.

Table 5-20 shows the maximum simulated aquifer concentrations for Pu-238 and Pu-239 for the plutonium mobile fraction. These values are all at least two orders of magnitude greater than the maximum observed concentrations. A contour plot of simulated aquifer concentrations at the 12-m (39-ft) depth for the smallest mobile fraction simulation is shown in Figure 5-62. Even with the 1×10^{-6} fractional release, the predicted aquifer concentrations at the current time in most of the locations sampled with aquifer wells would be greater than 0.1 pCi/L. Because most of the sample results are nondetects and the detects are generally just at the instrument detection limit of 0.01 to 0.02 pCi/L, these mobile fraction simulations do not mimic concentrations observed in the aquifer. Therefore, if a small mobile fraction does exist, it must be considerably smaller than the 1×10^{-6} fractional release modeled in this analysis. Otherwise, it should be much easier to detect plutonium in the aquifer.

Table 5-20. Maximum 12-m (39-ft) depth simulated Pu-238 and Pu-239 aquifer concentrations (pCi/L) through calendar year 2001 for the base simulation and the plutonium mobile fraction sensitivity simulations.

Contaminants of Potential Concern	Baseline Risk Assessment, No Mobile Fraction	Mobile Fraction 1×10^{-6}/year	Mobile Fraction 1×10^{-4}/year	Mobile Fraction 1×10^{-2}/year	Range of Observed 3σ Concentrations in the Subsurface Disposal Area Vicinity Wells Since 1987
Pu-238	0	$8 \times 10^{+1}$	$8 \times 10^{+3}$	$8 \times 10^{+5}$	0.018 to 0.37
Pu-239	5×10^{-28}	$4 \times 10^{+2}$	$4 \times 10^{+4}$	4 x 10*	0.094 to 4.3

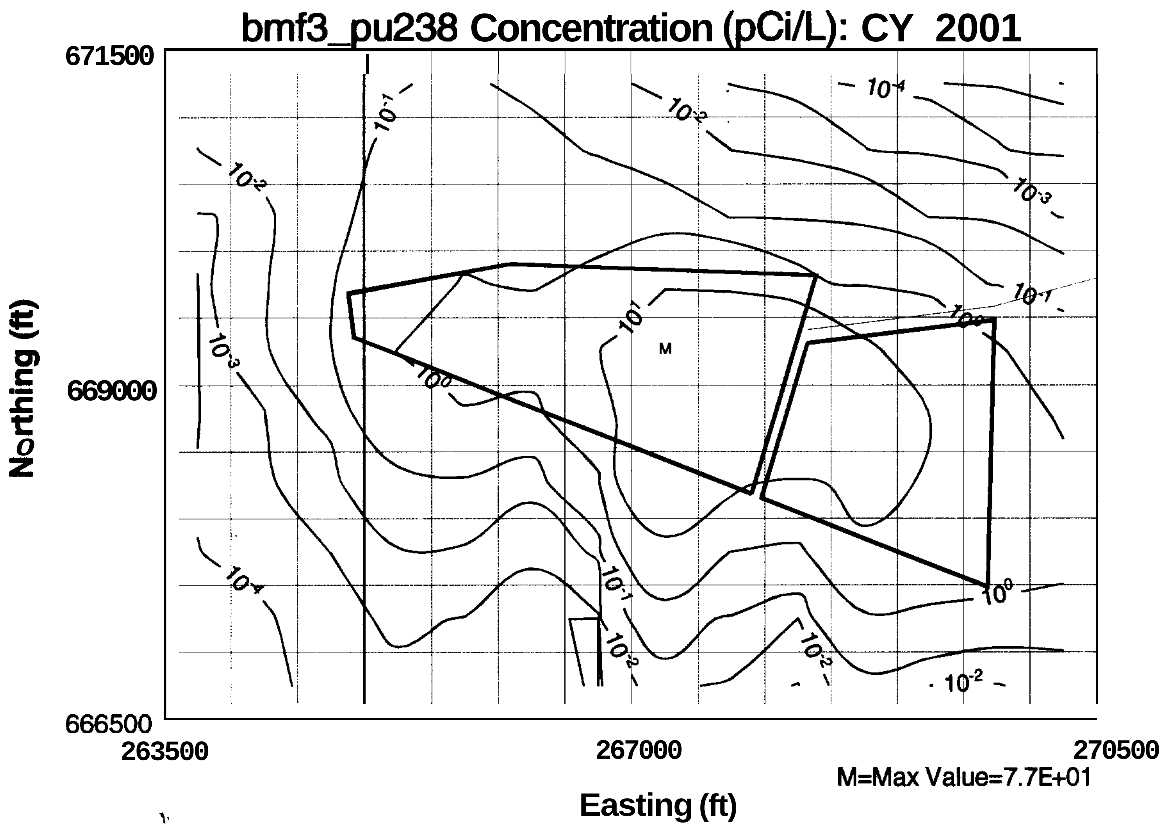

Figure 5-62. Simulated 12-m (39-ft) depth Pu-238 and Pu-239 aquifer concentrations (pCi/L) at calendar year 2001 for the simulation with a 1×10^{-6} mobile fraction.

Table 5-21 shows maximum simulated plutonium soil concentrations in the B-C interbed for comparison to those presented previously in Table 5-19 for plutonium K_d sensitivity simulations. Simulated interbed plutonium soil concentrations are approximately 1 to 7 orders of magnitude greater than results for the K_d sensitivity simulations. Except for the 1×10^{-6} mobile fraction, the results also significantly qver predict the maximum observed B-C interbed soil concentrations. Contour plots of the interbed soil concentrations are not included because they look similar to those for the K_d sensitivity results but with higher concentrations.

The conclusion from the interbed results for the mobile fraction is slightly different than that for the aquifer. Aquifer results precluded any of the simulated mobile fractions as being plausible, while the lowest mobile fraction does not, at least, contradict the observed interbed soil concentrations.

Table 5-21. Simulated maximum Pu-238 and Pu-239 B-C interbed soil concentrations (Ci/g) through calendar year 2001 for the base simulation and the plutonium mobile fraction sensitivity simulations.

Contaminants of Potential Concern	Base Simulation No Mobile Fraction	Mobile Fraction 1E-06/year	Mobile Fraction 1E-04/year	Mobile Fraction 1E-02/year	Maximum Sampling Results
Pu-238	7E-18	3E-13	3E-11	3E-09	1E-13
Pu-239	2E-16	3E-13	3E-11	3E-09	1E-12

5.2.6.5 Uranium Solubility. This sensitivity study was limited to changes in the source term release. No changes were required in the subsurface flow and transport models. Results are discussed in terms of risk in Section 6.

5.2.6.6 Neptunium Solubility. This sensitivity study was limited to changes in the source term release. No changes were required in the subsurface flow and transport models. Results are discussed in terms of risk in Section 6.

5.2.6.7 Spreading Area Influence. Two different simulations were implemented to test the effects of including additional water from the spreading areas. The implementation of these two simulations was discussed in Section **5.2.4.5.** One simulation set had no additional water added at depth, and one had four times as much water added so that the whole region of the C-D interbed beneath the SDA was affected by spreading-area water. For each of these cases, the entire suite of **COPCs** was simulated. These cases represent conceptual uncertainty bounds on the possible effects of the additional spreading-area water in the vadose zone. The case without the spreading area influence is the most comparable to the IRA model because that model also did not include any effect from the spreading area.

In both simulation sets, the amount of water exiting the bottom of the vadose zone was also input into the aquifer model along with contaminant masses. Additional spreading-area water entering from the vadose zone, coupled with the low-permeability region, results in dilution of simulated concentrations in the extreme western part of the refined portion of the aquifer.

5.2.6.8 Uniform Subsurface Disposal Area Infiltration Rates. Water infiltration rates are assigned at the upper boundary of the vadose zone simulation domain. These amounts of water also are input into the source term model and impact the contaminant release. Two simulation sets were performed to investigate the sensitivity of the simulated flow and transport to these assigned infiltration rates. Both simulation results are presented in terms of risk in Section 6.

In the first set, a uniform infiltration rate of 8.5 cdyear (3.3 in./year) was assigned instead of the spatially varying rate that was used in the ABRA simulation. This uniform infiltration rate was assigned beginning in **1952.** This simulation tested the impact of the detailed spatially variable infiltration assignment and included the three historical transient flooding events. The discussion of the impact on risk is included in Section 6. Figure 5-63 shows the simulated vadose zone water travel times with a uniform 8.5 cdyear (3.3 in./year) infiltration rate inside the SDA. These travel times are slightly longer than the ABRA simulated vadose zone water travel times discussed previously. The ABRA travel times ranged from **14** to 30 years at grid blocks contained entirely within the SDA boundary. By comparison, with the 8.5-cdyear (3.3-in./year) uniform infiltration rate, the travel times for the same grid blocks range from **17** to 38 years.

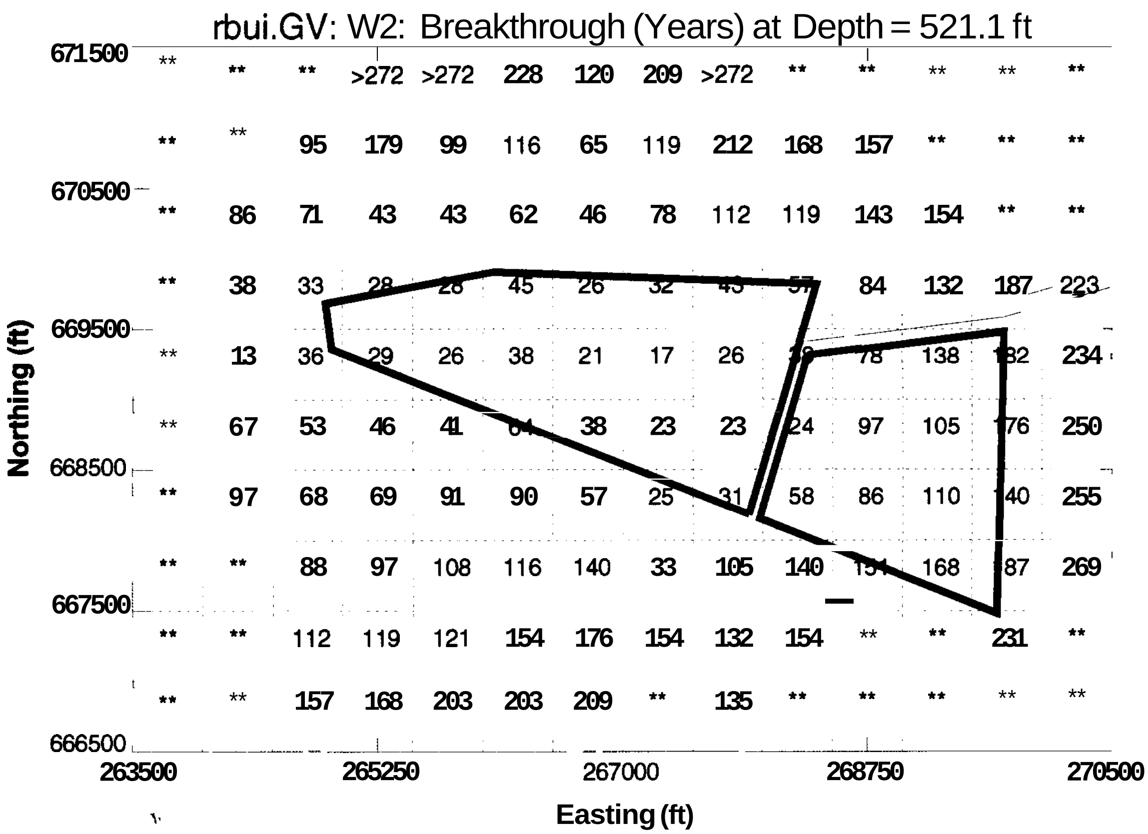

Figure 5-63. Simulated vadose zone water travel times (years) with a uniform infiltration rate of 8.5 cdyear (3.3 in./year) inside the Subsurface Disposal Area.

The second simulation set had a uniform infiltration rate of 23 cm/year (9 in./year) applied inside the SDA, which is equivalent to the total average annual precipitation infiltrating into the subsurface with no loss to evaporation. This infiltration rate was assigned beginning in 1952. This 23-cm/year (9-idyear) infiltration rate was approximately a factor of three times greater than that in the ABRA simulation and can represent the possible effect of a change in climate that resulted in three times as much precipitation at the **INEEL,** Yet another way to consider this simulation is as a surface treatment being applied that ensured that the total precipitation currently received on the **INEEL** infiltrated into the subsurface and no portion of that water evaportranspirated back into the atmosphere.

5.2.7 Simulation Npmenclature

Given the extensive number and types of simulations performed for the ABRA, development of a nomenclature to track the simulations was necessary. This nomenclature section is included to allow the reader to recognize headings in the simulation results figures.

The contaminants, **as** they were divided into seven groups for purposes of performing the simulations, are described in Section 5.1.4 and listed in Table 5-6. Table 5-22 provides the nomenclature for the leading character string in the run names. The first letter is always a "b" for a BRA-related simulation. Table 5-23 shows how these conventions were applied to define names for each of the simulation groups. The table gives the application that was being simulated and a detailed description of the simulation group. The "grp*" indicates Groups 1 through 7, as appropriate for each name.

Table 5-22. Run-naming nomenclature.

Run Nomenclature	Run Description
Leading b	Baseline risk assessment
kd	K_d
mf	Mobile plutonium fraction
us	Uranium solubility
nps	Neptunium solubility
nsa	No spreading area influence
2sa	Twice spreading area
ui	Uniform 8.5 cm/year infiltration rate
ui2	Uniform 23 cm/year infiltration rate
gap	B-C interbed gap

Table 5-23. Simulation group names and descriptions.

Simulation Group Name	Application	Description
	NO ACTION	
b_grp*	Baseline risk assessment (BRA) base case	Best-estimate inventories, average infiltration = ***8.5*** cdyear, plutonium K_d = 5,100 mL/g. No mobile fraction, uranium solubility = 5.9E-04 g/cc, neptunium solubility = 7.5E-08 g/cc. Spreading areas do have influence on transport.
	NO ACTION SENSITIVITY: Hold all values constant as in BRA base case except as noted:	
bub_grp*	Upper-bound inventories	Upper-bound instead of best-estimate inventories.
bkd1_grp*, **bkd2_grp*,bkd3_grp***	Plutonium K_d	Three K_d values each for Groups 2 and **4** (K_d = 22,320, and 1,700).
bmf1_grp*,bmf2_grp*,bmf3_grp*	Plutonium mobile fractions	Three mobile fractions each for Groups 2 and **4** (mobile fraction = 1E-02, 1E-04, and 1E-06).
bus1_grp*,bus2_grp*,bus3_grp*	Uranium solubility	Two masses for Group ***5*** (mass = 9.3E-07 g/cc and 9.3E-11 g/cc).
bnps1**_grp*,bnps2_grp***	Neptunium solubility	Two masses for Group 1 (mass = 1.3E-11 g/cc and 1.2E-06 g/cc).
bnsa_grp*,b2sa_grp*	Spreading area influence	No influence and double the ABRA base case influence for Groups 1 through 7.
bui_grp*,bui2_grp*	Uniform Subsurface Disposal Area (SDA) infiltration	Uniform infiltration rates inside the SDA of ***8.5*** cdyear and 23 cdyear.
bgap_grp*	Gaps included in BC interbed	Gaps included in B-C interbed in grid blocks where any wells show zero thickness.
	Retrieval	Removal of all contaminant mass in surficial sediments, necessary for assessing potential contamination in the vadose zone.

5.3 Volatile Organic Compound Modeling

This section addresses VOCs, which have the added complication of being able to exist and be transported in a gaseous phase, Unlike dissolved-phase contaminants, which were simulated with an updated model since the IRA, no new modeling of VOCs has been performed for the ABRA. Instead, modeling for VOCs has been deferred to future activities planned for OU 7-08, the OCVZ Project. The IRA modeling results, with some adjustment to account for different inventories, were incorporated into this ABRA. Using the IRA results for VOCs is appropriate from the standpoint that modeling with new inventory estimates would not change the risks considerably. This section discusses the results of the IRA VOC modeling, the revised VOC COPC inventory estimates, and how both were used to estimate media concentrations for the ABRA.

5.3.1 Interim Risk Assessment Volatile Organic Contaminant Modeling and Results

The IRA VOC model is documented in Magnuson and Sondrup (1998). At its publication, it was the most comprehensive model developed for predicting water and contaminant movement in the SDA subsurface. The model included spatially variable lithology and time-dependent, spatially-variable infiltration in an integrated vadose zone-saturated zone (aquifer) representation. Contaminants were transported primarily by advection and diffusion in aqueous and gaseous phases. The model was implemented using the numerical simulation code TETRAD. Time-dependent releases of VOCs were calculated external to the TETRAD simulator using the DUST-MS code.

The vast majority of VOCs in the SDA subsurface were released from Rocky Flats Plant 743-series sludge. The sludge was prepared in an organic waste treatment processing facility at the Rocky Flats Plant by mixing lathe coolant (liquid carbon tetrachloride and Texaco Regal Oil) with calcium silicate. Small amounts of miscellaneous oils and other VOCs (e.g., tetrachlorethylene, trichloroethylene, and 1,1,1-trichloroethane) were also sometimes added. The resulting mixture was a very thick pasty substance devoid of free liquids. Because of the viscous nature of the 743-series sludge, it is unlikely that the VOCs were released or migrated as free liquids. Thus, VOC release by diffusion was simulated using DUST-MS. However, for computational convenience the VOCs were initially entered into the TETRAD model as free liquids, then quickly partitioned into aqueous- and vapor-phase components. Migration as a free liquid was not simulated, which is consistent with monitoring results because non-aqueous phase liquids have not been detected in vapor, perched water, or the aquifer.

The IRA VOC transport model was calibrated using carbon tetrachloride concentrations in soil gas, and aqueous concentrations in the aquifer and perched water. Calibration consisted of simulating the release and migration of VOCs until modeled concentrations matched actual concentrations within some specified tolerance. Initially, the HDT (LMITCO 1995) best-estimate carbon tetrachloride inventory value of 113,000 kg (250,000 lb) was used in the calibration. However, this inventory was insufficient to achieve adequate calibration despite relaxing other model parameters. To improve the calibration, the inventory was arbitrarily doubled to 226,000 kg (497,200 lb), and a much better match was obtained. However, it required that nearly all of the carbon tetrachloride be released in order to achieve calibration. Specifically, the IRA model assumed that 213,000 kg (468,600 lb) (94%) of the 226,000 kg (164,200 lb) of the carbon tetrachloride had been released by 1995, the end of the IRA calibration period. Of the 213,000 kg (468,600 lb) released by 1995, approximately 168,000 kg (369,600 lb) (79%) were predicted to have been lost to the atmosphere through vapor diffusion or advection, and 45,000 kg (90,000 lb) (21%) remained in the vadose zone.

In response to suspicions that the carbon tetrachloride inventory was too low, the inventories for the other organic COPCs (i.e., tetrachloroethylene and methylene chloride) also were doubled for the IRA. This made sense for tetrachloroethylene because it was codisposed with carbon tetrachloride in the

743-series sludge. Conversely, methylene chloride was not a component of 743-series sludge, but it did come from RFP as did the 743-series sludge. Therefore, doubling the methylene chloride seemed appropriate and fit with the intent of the IRA to be conservative.

The IRA model calibration was rather good in terms of agreement between modeled and measured concentrations of carbon tetrachloride. However, the model did not consider chemical degradation. Degradation is likely occurring based on detections of chloroform (a degradation byproduct). The IRA model did not include degradation because of uncertainty regarding the rate and mechanism. Neglecting degradation is conservative because byproducts of carbon tetrachloride degradation (i.e., chloroform, methylene chloride, and chloromethane) have transport properties similar to carbon tetrachloride, yet they all are less toxic (i.e., have higher risk-based concentrations).

Results of the IRA VOC model predicted VOC concentrations in soil and surface gas fluxes would peak shortly after burial. Soil concentrations and gas fluxes were used to calculate ingestion and inhalation risk. The VOC concentrations in groundwater were predicted to peak after the 100-year institutional control period at levels well above MCLs. Predicted maximum concentrations of VOCs in soil and groundwater as presented in the IRA are provided in Table 5-24 (Becker et al. 1998).

Table 5-24. Maximum predicted soil and groundwater concentrations for volatile organic contaminants of potential concern quantitatively evaluated in the Interim Risk Assessment.[a]

Contaminant of Potential Concern	Predicted Maximum Soil Concentration (mg/kg)	Year of Predicted Maximum Soil Concentration	Predicted Maximum Groundwater Concentration (μg/L)	Year of Predicted Maximum Groundwater Concentration
Carbon tetrachloride	1.65E+00	1967	304	2106
Methylene chloride	1.61E-02	1967	487	2187
Tetrachloroethylene	4.70E-01	1968	127	2138

a. Concentrations and dates were calculated from model results using a 30-year running average (Becker et al. 1998).

5.3.2 Revised Volatile Organic Compound Inventory Estimates

The IRA VOC modeling indicated that the best-estimate inventory as presented in the HDT was too low for carbon tetrachloride, which led to a two-part investigation that ultimately resulted in an estimate for carbon tetrachloride that was several times higher than the HDT value. The initial investigation by Miller and Navratil (1998) evaluated monthly shipping records rather than yearly records as had been done in the past. Miller and Navratil (1998) also used newly acquired information on the makeup of 743-series sludge and concluded that the carbon tetrachloride inventory could be approximately 4× the HDT value. The follow-on investigation by Miller and Varvel (2001) made use of other critical sources of information (e.g., RFP Building 664 waste disposal sheets and the RFP Building 774 Organic Waste Treatment Process Logbook) that were obtained as a result of inquiries made by Miller and Navratil (1998). These other sources of information allowed an even more accurate count of the 743-series sludge drums buried in the SDA. Miller and Varvel (2001) estimated that the carbon tetrachloride mass in the 743-series sludge was 8.2E + 05 kg, which is approximately 7.3× more than the best-estimate value in the HDT.

Miller and Varvel (2001) also estimated total VOC mass in 743-series sludge to be 1.0E + 05 kg. From that estimate, Varvel (2001) calculated the mass of the other VOCs in 743-series sludge: trichloroethylene, tetrachloroethylene, and 1,1,1-trichloroethane. Lacking any evidence to the contrary, Varvel (2001) assumed the VOC mass that was not carbon tetrachloride consisted of equal volumes of the other three VOCs. This resulted in an estimated mass of 9.8E + 04 kg of tetrachloroethylene, or about 3.9× more than in the HDT estimate. Varvel (2001) also investigated methylene chloride, which is not a component of 743-series sludge, and concluded that the methylene chloride inventory presented in the HDT was reasonable and appropriate.

Table 5-25 contains a summary of the VOC COPC inventories. The table shows that the revised best-estimate inventory for carbon tetrachloride and tetrachloroethylene is greater than the HDT inventory and even greater than the IRA inventories, which were double the HDT values. The current best-estimate inventory for methylene chloride, the other organic COPC, has not changed from the value used in the HDT. Therefore, the inventory for methylene chloride used in the ABRA is the same inventory reported in the HDT (LMITCO 1995a) value, or one-half the IRA value.

Table 5-25. Summary of volatile organic compound contaminant of potential concern inventories.

Contaminant of Potential Concern	Original Best-Estimate Inventory[a] (kg)	IRA Inventory[b] (kg)	Revised Best-Estimate Inventory (kg)	Ratio of Revised to Original" Best-Estimate Inventory	Ratio of Revised to IRA Inventory
Carbon tetrachloride	113,000	226,000	820,000[c]	7.3	3.6
Tetrachloroethylene	25,000	50,000	98,000[d]	3.9	2.0
Methylene chloride	14,000	28,000	14,000[d]	1 (no change)	0.5

a. Taken from *A Comprehensive Inventory of Radiological and Nonradiological Contaminants in Waste Buried in the Subsurface Disposal Area of the INEL RWMC During the Years 1952–1983* (LMITCO 1995).
b. Interim Risk Assessment (Becker et al. 1998) with modeling in Magnuson and Sondrup (1998). The IRA inventory is 2× the original best-estimate inventory.
c. *Reconstructing Past Disposal of 743 Series Waste in the Subsurface Disposal Area for Operable Unit 7-08, Organic Contamination in the Vadose Zone* (Miller and Varvel 2001).
d. Varvel (2001)

5.3.3 Implications of Revised Volatile Organic Compound Inventories

The IRA inventories and ABRA revised best-estimate inventories are different for the VOC COPCs; therefore, it is reasonable to assume that media concentrations (soil, groundwater) and surface gas fluxes would be different. Information from a previous modeling study was used (Sondrup 1998) to appropriately scale the IRA results to the new ABRA revised best-estimate inventory. Before completion of the carbon tetrachloride inventory investigation by Miller and Varvel (2001), Sondrup (1998) performed some preliminary modeling of carbon tetrachloride transport. At the time, Miller and Varvel (2001) were confident that the carbon tetrachloride inventory would be at least 5× greater than the best estimate reported in the HDT. Sondrup then evaluated potential groundwater impacts assuming a preliminary carbon tetrachloride inventory of 5× the HDT (LMITCO 1995a) value, or 2.5× greater than the IRA value. While complete details of the study are documented in Sondrup (1998), relevant information has been included here.

Sondrup (1998) modeled carbon tetrachloride using essentially the same model as the IRA VOC model documented in Magnuson and Sondrup (1998), with some modifications. The major modification used a smaller model domain and increased grid refinement in the vertical dimension. These changes were enacted to speed simulation times and increase resolution in the vicinity of the SDA. The drawback was that the new domain did not extend to the INEEL boundary; therefore, concentrations at the boundary could not be predicted with the model.

Because of modifications to the IRA model and the larger source inventory of carbon tetrachloride, it was decided that the model should be recalibrated. To limit the effort required for recalibration, it was decided that all source-release parameters could be modified to make the release rate using the preliminary 5× inventory (i.e., 5× the HDT inventory) imitate the general release rate character of the IRA inventory (i.e., 2× the HDT inventory) during the period of IRA model calibration (1952 to 1995). The additional mass from the 5× inventory would then be released after the calibration period. Figure **5-64** illustrates a comparison of the release rate for the IRA and 5× sources. The IRA and 5× results are similar in trend with one major difference: A few years before the end of the calibration period, virtually nothing is being released from the IRA source, while the 5× source is still active. This can be seen more dramatically in Figure 5-65, which compares the cumulative release of the IRA and 5× sources. At approximately the year 2000, virtually nothing is left in the IRA source, while the cumulative release from the 5× source continues to increase.

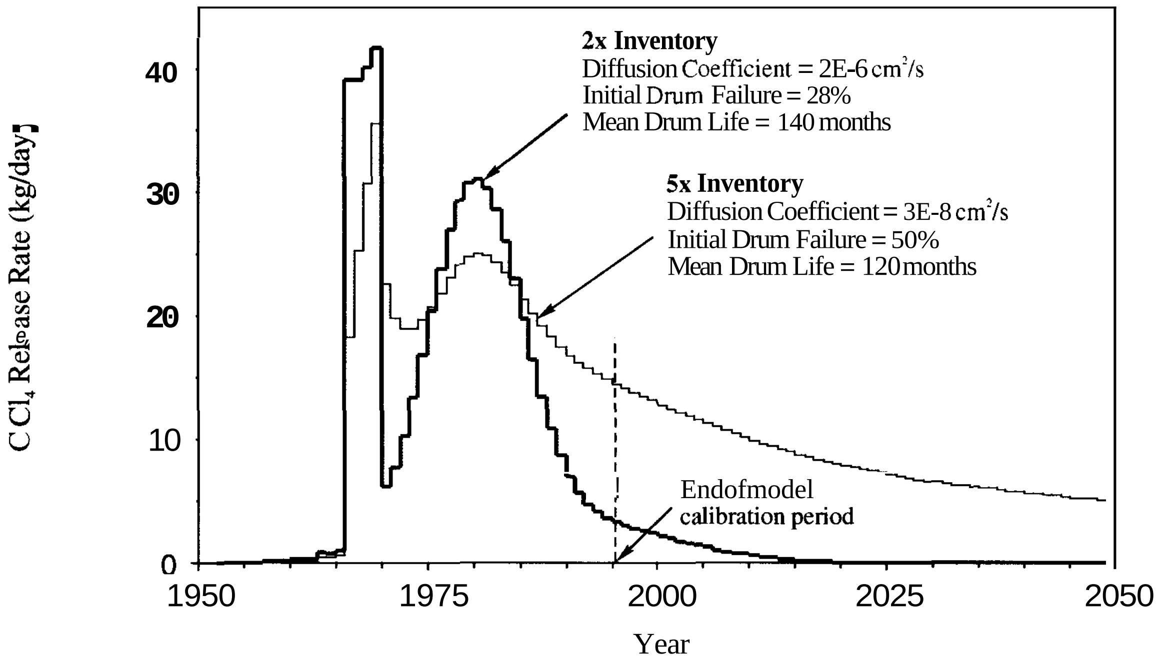

Figure **5-64.** Comparison of carbon tetrachloride release rates using the Interim Risk Assessment inventory (2×) and the preliminary 5× inventory estimate.

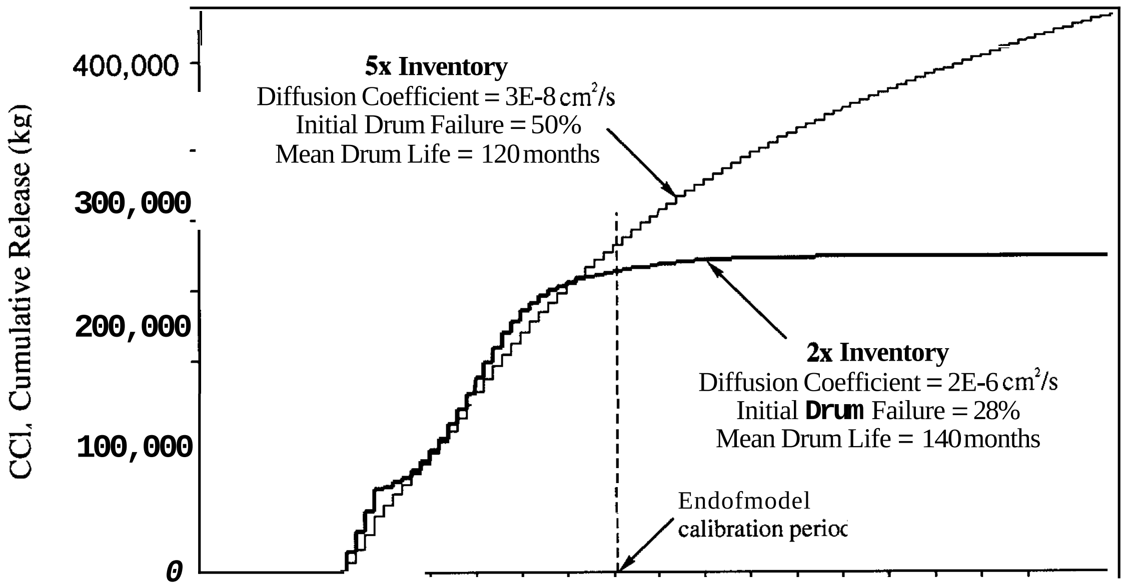

Figure 5-65. Comparison of carbon tetrachloride cumulative release using the Interim Risk Assessment inventory (2×) and the preliminary 5× inventory estimate.

Figure 5-66 compares carbon tetrachloride concentrations in groundwater at the southern boundary of the SDA for the IRA and 5x inventories, as predicted by the Sondrup (1998) model. The predicted peak concentration for the recalibrated model using the IRA inventory is 337 µg/L and occurs in calendar year 2110, while the peak concentration for the 5x inventory is 740 µg/L and occurs in calendar year 2165, over 50 years later. The recalibrated model using the IRA inventory is close to the result using the original IRA model (304 µg/L) published in Magnuson and Sondrup (1998). The difference is attributable to modifications made to the IRA model and to the new calibration of the VOC model from Sondrup (1998).

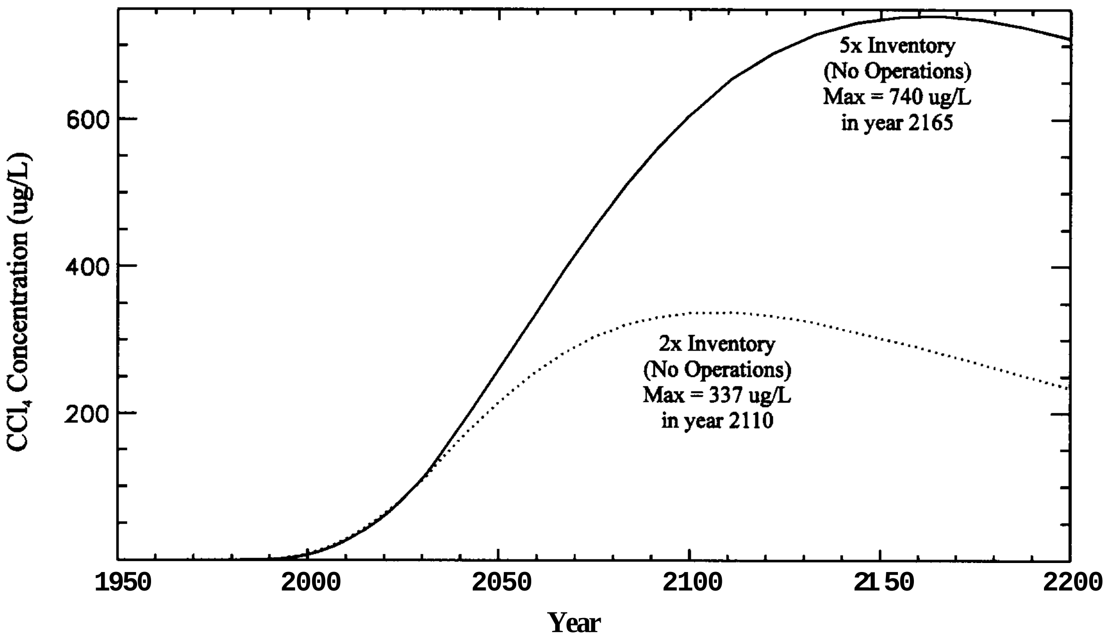

Figure 5-66. Comparison of simulated carbon tetrachloride concentrations in the aquifer near Well M10S for the Interim Risk Assessment and revised inventory estimates.

Results show that the 5x inventory (which is 2.5x larger than the IRA inventory) produced a peak groundwater concentration 2.2x larger than the IRA inventory. While the results are not a direct 1:1 correlation, they are close enough that a 1:1 correlation is reasonable and appropriate in light of the uncertainties. Therefore, because the ABRA revised best-estimate inventory is 3.6x larger than the IRA inventory, it is appropriate to assume that peak groundwater concentration from the ABRA revised best-estimate inventory could be 3.6x larger than the IRA peak concentration, or 1,094 µg/L (3.6 x 304 µg/L). This value should be thought of as an upper-bound estimate of peak concentration based on the following logic. The IRA inventory can be considered the minimum amount necessary to generate the carbon tetrachloride plume as observed in 1995. This is because it was necessary to release essentially all of the IRA inventory before 1995 and also use fairly extreme values for key model parameters to keep enough contamination in the subsurface to recreate the observed plume. When simulating the 5x inventory (Sondrup 1998), all additional mass above the minimum amount necessary to generate the plume was released after the calibration period because the release rate was essentially the same as the IRA model up to 1995, This additional mass, coupled with the model parameters designed to keep mass in the subsurface, produces high groundwater concentrations. These high groundwater concentrations can be considered upper-bound impacts to groundwater because if the same model parameters that were adjusted to keep mass in the subsurface were conversely relaxed, more mass would escape to the atmosphere, meaning a larger inventory could be tolerated by increasing the release rate. This, in turn, would reduce impact to groundwater.

Assuming a **1:1** correlation between inventory and peak groundwater concentration, groundwater impacts for the other VOC COPCs were estimated by scaling the IRA modeling results using a ratio of the ABRA revised best-estimate inventory to the IRA inventory. Table **5-26** contains estimated peak groundwater concentrations for the three VOC COPCs.

Table **5-26.** Estimated peak groundwater concentrations for revised inventories of volatile organic compound contaminants of potential concern.

Contaminant of Potential Concern	Interim Risk Assessment[a] Peak Groundwater Concentrations (µg/L)	Ratio of Ancillary Basis for Risk Analysis Revised Best-Estimate Inventory to the Interim Risk Assessment[a] Inventory	Estimated Peak Groundwater Concentrations (µg/L)
Carbon tetrachloride	*304*	**3.6**	1094
Methylene chloride	487	0.5	244
Tetrachloroethylene	127	2.0	254

a. Interim Risk Assessment (Becker et al. 1998) concentrations were calculated using a 30-year running average.

Though the predicted peak groundwater concentration occurred later in time for the Miller and Varvel **(2001)** inventory simulation when compared to the IRA simulation, the ABRA simply used scaled **IRA** results without regard to timing.

Soil concentrations and surface gas fluxes used to calculate ingestion and inhalation risks also were scaled based on the inventory ratio. This is likely a more conservative approach than it was for groundwater because the surface soil concentrations and surface fluxes are very closely tied to release rates. Because the 5× release rate was made to look similar to the IRA release rate (see Figures **5-64** and 5-65), it can be expected that the soil concentrations and surface fluxes are also similar. However, given that the release rate could have been higher for a larger inventory, as discussed previously in this section, it is reasonable that soil concentrations and flux results also can be scaled using the inventory ratio.

5.3.4 Impact of Vapor Vacuum Extraction on Volatile Organic Compound Concentrations

In January **1996,** OU 7-08 began operation of a multi-well VVE system inside the SDA to remove gas-phase VOCs from the subsurface. This system has operated on a nearly continuous basis since **1996** and removed more than **45,000** kg (**99,000** lb) of total VOCs from the subsurface.

Estimated concentrations and fluxes discussed in the previous section are base case estimates, taking no account for remedial actions such **as** those performed for OU 7-08. Operation of the VVE system has reduced vadose zone soil gas concentrations and perched water concentrations considerably in many locations and will certainly reduce future impacts to groundwater; however, the full extent is not known at this time. Also, it appears that sufficient mass may be remaining in both the source and vadose zone (Sondrup **1998)** to necessitate continued operation of the VVE system in order to meet the OU 7-08 ROD objectives. Therefore, OU 7-08 will continue to monitor VOC concentrations and predict plume development caused by operation of the VVE system and future releases.

5.4 Biotic Transport

The biotic pathway model predicts the transport of contaminants to the surface through plant intrusion or animal burrowing. Selection of DOSTOMAN for the biotic pathway model for the ABRA is detailed in Becker (1997). The following subsections describe how the DOSTOMAN code was used to predict surface concentrations of contaminants at the SDA.

Unlike other WAGs, the contaminants at WAG 7 are buried under an average of 1.5 m (5 ft) of soil cover. The contaminants must be brought to the surface to enable human contact with contaminants. One possible mechanism for the contaminants to be brought to the surface is biotic transport, which has been measured at the INEEL. The 1.5-m (5-ft) soil cover at WAG 7 is not deep enough to prevent intrusion into the waste by the deeper burrowing animals and rooting plants; therefore, biotic transport was modeled for WAG 7.

5.4.1 Biotic Model Methodology

The DOSTOMAN code was used to predict the amount of contaminants brought to the surface. Yearly average concentrations were computed for the SDA. Four successive phases have been addressed that describe transition from the current disturbed setting back to a native vegetation mixture. The processes modeled using DOSTOMAN include animal burrowing, burrow collapse, plant uptake, radioactive decay, and leaching of contaminants from infiltrating water. Loss caused by erosion or surface runoff was not modeled. Neglecting erosion and surface runoff is conservative because it leads to higher surface concentrations at the SDA. The effect of including erosion would be to remove contaminant mass from the surface and, thereby, reduce the soil concentration to which the receptor would be exposed. The effect would be offset by the reduced depth to the waste and the enhanced intrusion. However, the erosion scenario is not appropriate for the SDA because it is a depositional environment (Hackett et al. 1995).

The SDA has been used for shallow land disposal since 1952. The possibility exists that animals and insects on or adjacent to the SDA could serve as mechanisms of transport or accumulation of contaminants at the surface. The DOSTOMAN code was used to simulate the movement of contaminants by plant uptake, as well as animal and insect excavation, to evaluate the transport of contaminants through biota. Release of nonvolatile contaminants to the surface environment involves mechanical transport of waste to the surface. The mechanical transport can be simulated using a compartmentalized model that provides for flora to uptake waste and burrowing animals to burrow into the waste and deposit it at the surface. The compartmentalized modeling approach has been used (Shuman, Case, and Rope 1985) to model the movement of radionuclides at the INEEL with the DOSTOMAN code (Root 1981).

Subsurface contamination at the SDA can be moved to the surface and near-surface soil profile through root assimilation. Once transferred to aboveground plant structures, contamination may be transported by primary consumers through the food web or accumulate in the surface soil through plant death and decay. Most of the SDA has been seeded with crested wheatgrass ***(Agropyron cristatum)*** to reduce moisture infiltration and erosion. Russian thistle (***Salsola kali***) has invaded disturbed areas that have not been seeded successfully with grass. The vegetation surrounding the SDA is dominated by big sagebrush ***(Artemisia tridentata)***, green rabbitbrush (***Chrysothamnus*** *viscidiflorus*), and bluebunch wheatgrass ***(Pseudoroegneriu spicatu).***

Redistribution of soil by burrowing animals may impact mobility of buried waste through transport enhancement, intrusion and active transport, and secondary transport (Arthur and Markham 1982; Cline et al. 1982). Four rodent species account for more than 90% of the composition of small mammals inhabiting the crested wheatgrass and Russian thistle habitat types at the SDA. These are Townsend's ground squirrel ***(Spermophilus townsendii***), **4%; Ord's** kangaroo rat (***Dipodomys ordii***), 10%; montane vole (Microtus *montanus*), 23%; and the deer mouse (*Peromyscus maniculatus*), 57% (Groves and Keller 1983).

Evidence exists that harvester ants ***(Pogonomyrmex salinus*)** are active at the **INEEL.** The sampling of harvester ant nests at TRA ponds suggests that the ants redistribute radionuclide concentrations in soil and the effect is seen mainly in the mound material (Blom, Johnson, and Rope 1991). In addition, harvester ants appear to have transported radioactive contaminants at the Boiling Water Reactor Experiment I site (Blom, Johnson, and Rope 1991) where a zone of surface contamination was covered with a layer of gravely soil at least 15 cm (6 in.) deep. Harvester ants also exhibit a preference for disturbed conditions similar to those found on the SDA (Fitzner et al. 1979; McKenzie et al. 1982).

The DOSTOMAN code mathematically simulates movement of contaminants from subsurface source compartments to overlying sink compartments by solving a system of differential equations at specified time steps. The general equation is shown below:

$$dQ_n / dt = \sum_{m=1}^{N} \lambda_{n,m} Q_m - \sum_{m=1}^{N} \lambda_{m,n} Q_n - \lambda_R Q_n \pm S_n \qquad (5\text{-}5)$$

where

Q_n = quantity of contaminant in compartment n (g)

Q_m = quantity of contaminant in compartment m (g)

$\lambda_{n,m}$ = rate constant for the transport of contaminants from compartment m to compartment n (year^{-1})

$\lambda_{m,n}$ = rate constant for the transport of contaminants from compartment n to compartment m (year^{-1})

λ_R = decay constant for the contaminant (year-')

S_n = source or sink term in compartment n (g/year)

N = total number of subsurface source compartments under consideration.

The first summation term in Equation (5-5) is the sum of all input rates to compartment n. The second summation term includes all rate-constant losses from compartment n. The remaining two terms include contaminant decay and the gain or loss in compartment n from sources or sinks.

At specified time increments, the system of differential equations presented by Equation (5-5) for n compartments can be solved to determine the contaminant inventory Q_n for each compartment. Details of the mathematical approach for determining a solution are given in Root (1981).

The DOSTOMAN model is represented graphically in Figure 5-67. Up to eight contaminants can be modeled in a single run. The figure shows only two components that are part of a single decay chain. This simplification was used to illustrate how the model was set up. The first contaminant mass is contained in the dotted blue box at the left of Figure 5-67. Waste zones are represented by the two red boxes at the bottom of the figure. Once mass is released from the waste by the source term model, the mass amount is input into the waste zones. Empty black boxes above the waste zone represent the

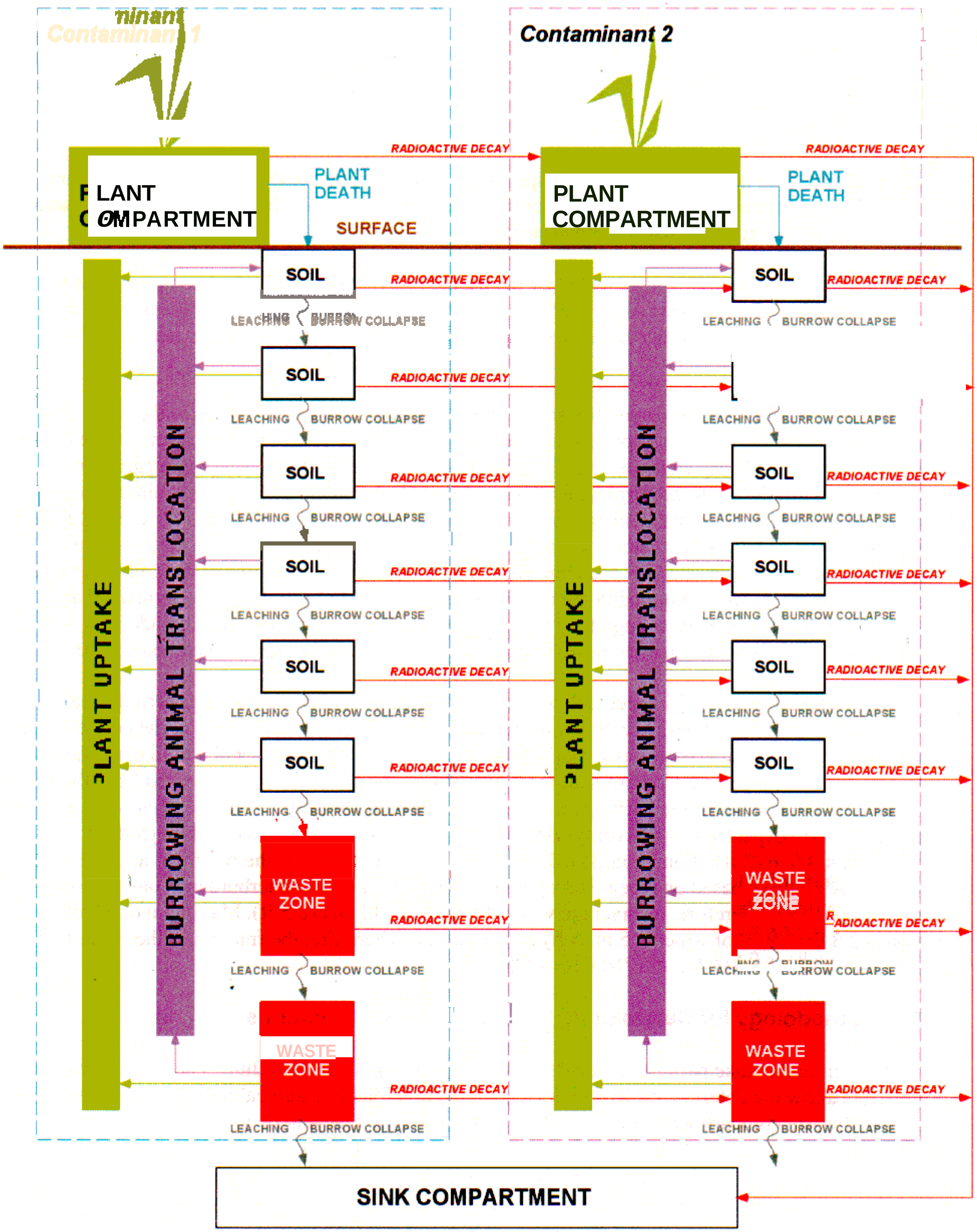

Figure 5-67. DOSTOMAN biotic modeling.

individual soil compartments. The green shaded box at the upper left corner is the plant compartment. Contaminant mass is assimilated by the plants and becomes part of the plant compartment, which is represented by the green lines that come from the waste zone and the individual soil zones to the plant compartment.

The mass of contaminant that is assimilated by plants is released when the plants die. Plant death is represented by the blue line from the plant compartment to the surface compartment. In reality, plant death contributes contaminant mass to all the soil compartments; however, for simplicity, the contaminant is shown as going only to the surface compartment.

Contaminant movement is represented by the purple line from the individual compartments to the surface compartment. Contaminant mass can be removed from an individual compartment by leaching or burrow collapse, which effectively moves mass to the next lower compartment and is represented by the gray lines in Figure **5-67.**

Radioactive contaminants decay. If a stable isotope decays, the lost mass goes to the sink compartment; that is, the stable isotopes are not hazardous and are no longer tracked. However, if another radioactive isotope in a decay chain decays, then the mass is transferred to the set of compartments seen on the right of Figure **5-67** (in the purple dotted box labeled Contaminant 2). The contaminant mass can be transported by all the same mechanisms as the original isotope. The transport rates are controlled by the properties (e.g., plant uptake factors or soil-to-water partition coefficient) of each isotope. The contaminant blocks were repeated for each contaminant modeled in a single simulation. Contaminants in any given compartment were assumed in the modeling to be available for transport by animals that burrow into a compartment even though they may not burrow as deeply as the waste. In addition, shallow-rooted plants were assumed to be able to uptake contaminants in nonwaste compartments.

Uptake of contaminants by sagebrush was not modeled during the occupational period because it was assumed that current RWMC operations would inhibit growth of sagebrush during the period of institutional control. It also was assumed that maintenance of the SDA surface soil would continue during the institutional control period. Contaminant mass available is 23.2% of the mass released from the source term model. This accounts for the burying of much of the waste more deeply than the plant roots or animal burrows are expected to go. Average depth to basalt is 5.3 m **(17.5** ft) with **1.5** m **(5** ft) of overburden and **0.6** m (2 ft) of underburden. The 1.5-m (5-ft) overburden is the weighted average of thickness of overburden based on recent survey results. The **0.6-m** (2-ft) underburden is based on current operational practices. Therefore, the average waste thickness is 3.2 m **(10.5** ft). Maximum depth of biotic intrusion is 2.3 m **(7.6** ft) of which **1.5** m (5 ft) is overburden. Therefore, the fraction of the waste that is available for uptake is 0.8/3.2 m (2.6/10.6 ft) or **25%.**

5.4.2 Methodology for Determining DOSTOMAN Rate Constants

Transport and uptake parameters are determined using applicable literature. The biotic transport rate constants allow the determination of radionuclide and nonvolatile chemical movement between the contaminated waste compartment and overburden compartments. The generic symbol for the rate coefficient for compartment n to compartment m is $\lambda_{m,n}$. The specific coefficients for each process are defined below. A superscript is used to identify the coefficients for an individual process such as plant uptake. For example, the plant uptake rate coefficient for compartment n to compartment m is λ_{mn}^{PU}. These coefficients are then used as shown in Equation **(5-1)** to determine soil contaminant concentrations. The plant death-rate constant determines the rate at which biomass dies and decays in the soil of each compartment. The rate constant is given by the following expression:

$$\lambda^{PD}_{m,n} = \sum_{i=1}^{N}[(1 - FBAG_i) \times FD_i \times FP_{i,m} + (FBAG_i \times FD_i)_{surface}] \tag{5-6}$$

where

$\lambda^{PD}_{m,n}$	=	death-rate constant for each plant in each compartment m (year-')
$FBAG_i$	=	fraction of total biomass of plant species i that is aboveground
FD_i	=	fraction of belowground biomass of plant species i that dies annually (year^{-1})
$FP_{i,m}$	=	fraction of belowground mass of plant i in soil compartment m
N	=	number of plant species.

The second term in this expression is used only in the uppermost (surface) soil compartment. This term accounts for aboveground biomass that is assumed to enter the uppermost soil compartment (surface) at a rate equal to the annual death rate. The second term is deleted for all other soil compartments. The death-rate constant is calculated for each plant species, which is then summed to give an aggregate death-rate constant for each soil compartment.

Data for plant death and plant uptake were compiled from both INEEL-specific and outside literature. All source references, data reviews, and compilations have been summarized in Hampton and Benson (1995) and Hampton (2001).

The current scenario reflects plant production over a period of 100 years, during which time the current vegetation community is maintained. Community composition for future scenarios was modeled for four separate periods to replicate change in community structure over time (e.g., 100 to 130, 130 to 150, 150 to 200, and greater than 200 years).

Plant-age composition for current and future scenarios was assumed to remain constant over the modeled periods. Biomass calculations were based on a total community production and fractional contributions of individual plant species (NRCS 1981). Successional trends of the SDA from the current vegetation community were assumed to result in a natural community similar to sagebrush-grass communities surrounding the RWMC and other parts of the region (Anderson 1991; Anderson and Inouye 1988; NRCS 1981).

Where possible, best-estimate input values from studies conducted in disturbed soil were used for the current scenario and values from undisturbed studies for 100+-year scenarios. Average values from studies with the greatest sample size were given preference and the largest average was selected if there were no differences in sample sizes. If no average was reported, a median value was calculated from a published range. Otherwise, the smallest reported maximum value from all studies was selected. Data specific to the INEEL were selected over off-Site data unless the study was flawed or somehow less applicable; for example, plants grown in media other than native soil.

5.4.3 Flora—Current Scenario

The vegetation cover on the SDA comprises two species: crested wheatgrass (Agropyron *cristatum*) and Russian thistle (*Salsola kali*) (Arthur and Markham 1982). Biomass and rooting depths for these species are summarized in Table 5-27. The total average community biomass (aboveground and belowground) was estimated as approximately **11,000** kg/ha (2.2 ton/ha) for current SDA conditions (Arthur and Markham **1982).**

Table 5-27. Fractional root distribution for individual plant species for the current scenario.

Depth (cm)	Crested Wheatgrass"	Russian Thistle"
Oto **15**	**0.35**	**0.22**
15 to **30**	**0.25**	**0.21**
30 to **45**	**0.10**	**0.21**
45 to **90**	**0.23**	**0.23**
90 to **135**	**0.04**	0.10
135 to **180**	**0.03**	**0.03**
180 to **225**	**0**	**0.02**
225 to **270**	**0**	0

a. Reynolds (1990).
Note: **Data in bold are specific to the Idaho** National **Engineering** and **Environmental** Laboratory.

The composition was assumed to remain constant through **100** years of maintenance of current conditions. Rooting depths and root mass distribution are summarized on Table **5-28.** The maximum rooting depth for crested wheatgrass is not expected to reach a depth sufficient to penetrate the waste matrix during the current scenario. However, Russian thistle can penetrate into the waste zone during the current occupational scenario. The establishment of sagebrush and other deeper rooting shrub species is controlled on the SDA; therefore, those species were not included as components for the current scenario.

5.4.4 Flora—100+-Year Scenario

The 100+-year scenario for vegetation consists of several phases in which transitional changes in the current SDA community composition result in reestablishment of a natural sagebrush and bunchgrass community (Anderson and Inouye **1988;** Anderson et **al. 1978;** NRCS **1981).** The composition of different species for communities modeled after **100** years is presented in Table 5-28, which summarizes the biomass and maximum rooting depth of the individual species for each transitional phase. Composition and percent biomass for successive increments are based on Arthur and Markham **(1982),** Anderson and Inouye **(1988),** Hull and Klomp (1974), Anderson et al. **(1978),** and Anderson **(1991).**

Table **5-28.** Fractional root distribution for individual plant species for the 100+-year scenario.

Depth (cm)	**Crested Wheatgrass"**	**Russian Thistle"**	**Sagebrush"**	**Green[b] Rabbitbrush**	**Bluebunch Wheatgrass[a]**	**Needle and Thread[a] Grasses**	**Other" Grasses**	**Forbs"**	**Other Shrubs[b]**
0 **to** 15	0.35	0.22	0.21	0.125	0.35	0.35	0.35	0.22	0.12
15 **to** 30	0.25	0.21	0.20	0.10	0.25	0.25	0.25	0.21	0.10
30 *to* 45	**0.10**	0.21	0.20	0.07	0.10	0.10	0.105	0.21	0.07
45 ***to* 90**	0.30	0.23	0.23	**0.45**	0.23	0.20	0.23	0.23	0.45
90 to 135	*0*	0.10	0.13	0.20	0.04	0.05	0.065	0.10	0.20
135 **to** 180	0	0.03	0.015	0.04	0.03	0.05	*0*	0.03	0.04
180 **to 225**	0	0	0.015	0.015	0	0	0	0	*0.02*
225 **to** 270	*0*	0	0	*0*	*0*	*0*	*0*	*0*	*0*

a. Reynolds (1990). Adjusted for maximum depths given on Table 5-28.
b. McKenzie et al. (1982).

Biomass calculations for the three periods (130 to 150, 150 to 200, and greater than 200 years) are based on average yearly above land-surface estimates of 1,490, 2,030, and 1,000 **kg/ha,** respectively (see Table 5-27). Root mass distribution with depth for this scenario is contained in Table 5-29. Sagebrush and similar shrubs (e.g., gray rabbitbrush [*Chrysothamnus nauseosus*]) are expected to attain maximum rooting depths with maximum shrub density developing at 200 years.

The other plant-rate constant is plant uptake, which simulates uptake of contaminants into the plant biomass. The death of the plants returns the contaminants to the soil compartments. The equation describing the uptake constant is shown in Equation (5-7).

$$\lambda_{m,n}^{P^U} = \sum_{i=1}^{N} (B_V \times PP_i \times FP_{i,m}) / MS_m \qquad (5\text{-}7)$$

where

$\lambda_{m,n}^{P^U}$ = plant uptake rate constant ($year^{-1}$)

B_V = plant bioaccumulation factor ([mg/g plant]/[mg/g soil])

PP_i = annual plant productivity (g/year) for all plants of species i

$FP_{i,m}$ = fraction of root mass of all plant species **i** in soil compartment m

MS_m = mass of soil in compartment m (g)

N = number of species.

The annual plant productivity (PP_i) can be found by using Equation (5-8):

$$PP_i = SB_i \times (RS_i + 1) \times FN_i \times SA \qquad (5\text{-}8)$$

where

PP_i = annual plant productivity

SB_i = shoot biomass per unit area for species i (g/m^2)

RS_i = root-to-shoot ratio for species i

FN_i = fraction of total biomass produced each year (1/year)

SA = surface area of the SDA (m^2).

Table 5-29. Estimated parameters for the uptake of plant species for the Subsurface Disposal Area for current and 100- to 200+-year scenarios.

Plant Species	Root-to-Shoot Ratio	Fraction Litterfall (Year⁻¹)[a]	Fraction Root Death (Year⁻¹)[b]	Current Scenario: Maximum Root Depth (cm)	Current Scenario: Fraction of Total Biomass'	100+-Year Scenarios: Maximum Root Depth (cm)	100+-Year Scenarios: Fraction of Total Biomass 130 Years[d]	100+-Year Scenarios: Fraction of Total Biomass 150 Years[d]	100+-Year Scenarios: Fraction of Total Biomass 200+ Years[d]
Crested wheatgrass	8"	**1**	0.5	**150'**	**0.75**	759	**0.55**	**0.30**	—
Russian thistle	1.4[b]	**1**	**1**	172[h]	**0.25**	172[h]	**0.15**	—	—
Sagebrush	**1.3**[e]	0.50'	0.5	—	—	220'	**0.05**	**0.10**	**0.20**
Green rabbitbrush	**1.3**[e]	0.85'	0.5	—	—	200'	**0.11**	**0.06**	**0.05**
Bluebunch wheatgrass	8"		0.5	—	—	150[j]	**0.03**	**0.05**	**0.10**
Needle and thread grasses	9'		**0.5**	—	—	139[j]	**0.02**	**0.09**	**0.10**
Other grasses	9'		***0.5***	—	—	100[f,j]	**0.05**	**0.20**	**0.29**
Forbs	1.5[b]		0.8[a]	—	—	145[h]	**0.02**	**0.10**	**0.15**
Other shrubs	1.5[b]		0.8[a]	—	—	183'	**0.02**	**0.10**	**0.11**
			Community aboveground biomass (kg/ha)	—	**1,490**	—	**1,490**	1,700	**800**
			Community root-to-shoot ratio	—	**6.35**	—	5.57	5.70	5.22

a. Estimate based on root-to-shoot and fractional root depths for grass and shrub species presented in Becker et al. (1994).

b. Becker et al. (1994).

c. Arthur (1982); Arthur and Markham (1982).

d. Composition and percent biomass based on successive increments based on data presented in Arthur (1982); Anderson and Inouye (1988); Anderson (1991).

e. Hull and Klomp (1974).

f. Reynolds and Fraley (1989).

g. Abbott, Fraley, and Reynolds (1991).

h. Klepper, Gano, and Caldwell (1985).

i. Pearson (1965).

j. McKenzie et al. (1982).

k. For gray rabbitbrush from Klepper et al. (1979).

Notes: Data in bold are specific to the Idaho National Engineering and Environmental Laboratory.

— = Plant species is not present for this scenario.

Mass of soil in compartment m (MS,) can be found by using the following equation:

$$MS_m = VC_m \times \rho \tag{5-9}$$

where

MS_m = mass of soil in compartment m

VC_m = volume of compartment m (cm^3)

ρ = density of soil (1.5 g/cm^3).

Plant uptake constants are determined for each plant species in each compartment and then summed to produce the aggregate uptake rate constant for that compartment.

Movement of contaminants by burrowing animals and ants requires soil transport rate constants. The equation describing calculation of the soil transport rate constant is as follows:

$$\lambda^{\beta}_{m,n} = \sum_{i=1}^{N} (I_i \times MB_i \times FNB_i \times FB_{i,m}) / MS_m \tag{5-10}$$

where

$\lambda^{\beta}_{m,n}$ = soil transport rate constant (year")

I_i = number of individual animals in species i

MB_i = mass of soil moved to the surface per individual by species i (g)

FNB_i = fraction of new burrows per year for species i ($year^{-1}$)

$FB_{i,m}$ = fraction of burrows of species i in soil compartment m

MS_m = mass of soil in compartment m (g)

N = number of species.

A soil transport rate constant is calculated for each compartment for each species that burrows in that compartment. Constants for each species are summed to produce the aggregate soil transport rate constant for each compartment. The predominant effect produced by this constant occurs when a burrowing animal digs directly into the waste and transports it to the surface.

Burrowing animals enhance waste transport through intrusion activities that move contaminants to the surface. The DOSTOMAN biotic transport model includes the contributions of both burrowing mammals and harvester ants. Data were compiled from SDA- and INEEL-specific and outside literature.

5.4.5 Fauna—Current Scenario

Composition of burrowing species, population density, burrow volumes, and average burrow depths reflecting estimated current burrowing activity at the SDA are shown in Table 5-30. Burrow distribution with depth for individual species is listed in Table 5-31. Burrow distributions with depth for the current scenario are based on average burrow depths and the soil profile was assumed to be disturbed. No animals are expected to attain burrow depths sufficient to exceed the current overburden thickness of 1.5 m (5 ft) (calculated average). The deepest average burrow depths are 1.4 m (4.5 ft) for harvester ants and 1.3 m (4.3 ft) for Townsend's ground squirrels (see Table 5-30). Species densities (see Table 5-32) are based primarily on previous studies of the **SDA** by Groves (1981), Groves and Keller (1983), Koehler (1988), Boone (1990), and Boone and Keller (1993). Burrow volume, depth, composition, and average population densities were assumed to remain constant for 100 years, assuming institutional controls maintain current conditions over that period (see Tables 5-31 and 5-32).

5.4.6 Fauna—100+-Year Scenario

The composition of the animal community for the 100^+-year scenario was altered to reflect changes as the vegetation community is transformed to simulate conditions at the Site if institutional controls were discontinued. The composition, burrow depth, volume, and density of species for the 100^+-year modeled periods are summarized in Table 5-33. The fractional burrow distribution for each individual species is presented in Table 5-33. Burrow distributions with depth for the 100^+-year scenario are based on average burrow depths and undisturbed soil profiles. While rodent populations fluctuate widely from year to year (Boone and Keller 1993), the population densities presented are average species compositions and population levels over time.

Leaching from a compartment is computed using the following equation:

$$\lambda^{L}_{m,m+1} = \frac{P}{\theta R T_m} \qquad (5\text{-}11)$$

where

$\lambda^{L}_{m,m+1}$ = leach rate coefficient for compartment m (year'')

P = net infiltration (m/year)

θ = volumetric moisture content (unitless)

R = contaminant-specific retardation coefficient (unitless)

T = thickness of compartment m (m).

Table 5-30. Small-animal density and burrowing parameters for the current scenario.

Burrowing Animal Species"	Population (Individuals per **Hectare)**[a]	Maximum Depth (cm)	Burrow Volume (L)	Number of New Burrows (per **Year**)[b]
Townsend's ground squirrel	**5**	**130'**	**9.4'**	0.75
Ord's kangaroo rat	**5**	**90'**	**7.3'**	**0.87**
Deer mouse	**17**	**50**[c]	**1.3'**	0.87
Montane and sagebrush voles	30	**40'**	**2.1'**	0.87
Great Basin pocket mouse	**15**	77[d]	**6.8**[d]	0.75
Western harvester ant	**13'**	138'	**2.4**[g]	0.1[e]

a. Mammal species composition and populations are based on studies conducted on the SDA by Groves (1981), Groves and Keller (1983), Koehler (1988), Boone (1990), and Boone and Keller (1993).

b. McKenzie et al. (1982).

c. Reynolds and Laundre (1988).

d. Landeen and Mitchell (1981).

e. Blom, Clark, and Johnson (1991).

f. Gaglio et al. (1998).

g. Fitzner et al. (1979).

Note: Data in bold are specific to the Idaho National Engineering and Environmental Laboratory.

Table 5-31. Burrow volume and fraction of volume excavated at depth by small animals for the current scenario.

Depth of Disturbed Soil (cm)	Townsend's Ground Squirrel[a]	Ord's Kangaroo Rat[a]	Deer Mouse[a]	Voles[a]	Great Basin Pocket Mouse[b]
	Fraction of Volume				
0 to 15	0.06	0.16	0.38	0.46	0.24
15 to 30	0.18	0.13	0.29	0.46	0.24
30 to 45	0.34	0.23	0.25	0.08	0.24
45 to 90	0.24	0.47	0.08	0	0.29
90 to 135	0.18	0	0	0	0
135 to 180	0	0	0	0	0
180 to 225	0	0	0	0	0
225 to 270	0	0	0	0	0
Total burrow volume (L)	9.4	7.3	1.3	2.1	6.8

a. Reynolds and Laundre (1988); Reynolds and Wakkinen (1987).

b. McKenzie et al. (1982).

Table 5-32. Small-animal density and burrowing parameters for the Subsurface Disposal Area 100+-year scenario.

Species[a]	Number per Hectare[a] Current/100^{+} Years	Average Depth (cm)	Burrow Volume (L)	New Burrows (Year^{-1})[b]
Badger	1/3	**180**[c]	**318.0**[b,d] (diameter = **30** cm, length = 450 cm)	**3**
Deer mouse	**17/30**	**24**[e]	**1.7**[i]	**0.87**
Great Basin pocket mouse	**15/25**	44.4[f]	**5.6**[i]	**0.75**
Least chipmunk	**3/8**	**17.5**[g]	**5.5**[g]	**0.75**
Montane and sagebrush voles	**30/10**	**23**[i]	**1.5**[i]	**0.87**
Northern pocket gopher	**7/7**	13.4[h]	5.5[h,d]	**0.75**
Ord's kangaroo rat	**8/5**	**34**[i]	**7.2**[i]	**0.87**
Rabbits	**8/20**	150	**87.0**[d] (length = **170** cm)	0.75
Townsend's ground squirrel	**5/5**	**128**[e]	8.2[e]	**0.75**
Western harvester ant	20[j]/36[j]	138[k]	**7.0**[l,d]	0.1

a. Compiled from Groves (1981), Groves and Keller (1983), Koehler (1988), Boone (1990), and Boone and Keller (1993) unless otherwise noted.
b. Lindzey (1976).
c. McKenzie et al. (1982).
d. Calculated from data presented in reference.
e. Reynolds and Wakkinen (1987).
f. Landeen and Mitchell (1981).
g. Laundre (1989a).
h. Winsor and Whicker (1980).
i. Reynolds and Laundre (1988).
j. Blom, Clark, and Johnson (1991).
k. Gaglio et al. (1998).
l. Fitzner et al. (1979).
Note: Data in bold are specific to the Idaho National Engineering and Environmental Laboratory.

Table 5-33. Burrow volume and fraction of volume excavated at depth by small animals for the 100+-year scenario in undisturbed soil.

Depth of Undisturbed Soil (cm)	Townsend's Ground Squirrel[a]	Ord's Kangaroo Rat[a]	Deer Mouse[a]	Voles[a]	Great Basin Pocket Mouse[b]	Northern Pocket Gopher[b]	Least Chipmunk[c]	Badger[b]	Rabbits[d]	Western Harvester Ant
	Fraction of Volume									
0 to 15	**0.08**	**0.21**	**0.32**	**0.46**	0.32	0.98	**0.48**	0.21	**0.17**	0.2 1
15 **to** 30	**0.18**	**0.29**	**0.68**	**0.54**	0.3 1	0.02	**0.52**	0.2 1	**0.17**	0.21
30 to 45	**0.08**	**0.14**	**0**	**0**	0.37	0	**0**	0.20	**0.17**	0.21
45 to 90	**0.11**	**0.36**	**0**	**0**	0	0	**0**	**0.19**	**0.17**	0.15
90 to 135	**0.55**	0	0	0	0	0.	**0**	0.10	**0.17**	0.12
135 to 180	0	0	0	0	0	0	**0**	0.09	**0.15**	0.10
180 to 225	0	0	0	0	0	0	**0**	0	**0**	0
225 to 270	0	0	0	0	0	0	**0**	0	**0**	0
Total burrow volume (L)[e]	**8.2**	**7.2**	**1.7**	**1.5**	5.6	5.5	**5.5**	170	**87**	2.4

a. Reynolds and Laundre (1988).
b. McKenzie et al. (1982).
c. Laundre (1989a; 1989b).
d. Wilde (1978).
e. Total burrow volumes from Appendix C, Table C-3.
Note: Data in bold are specific to the Idaho National Engineering and Environmental Laboratory.

Burrow collapse is computed using the burrow compartment mass excavation given in Equation (5-12). The lowest compartment receives mass from the middle compartment equal to the amount of soil moved to the surface from the lowest compartment. The middle compartment receives mass from the upper compartment equal to mass moved to the surface from both the first and second compartments. This way mass removed by burrowing is replaced by burrow collapse from the compartment above. Total mass moved into any compartment by burrow collapse is equal to mass removed from that compartment plus total mass moved to the surface from all compartments below. The equation for computing the burrow collapse for a compartment is shown in Equation (5-12):

$$\lambda^{c}_{m,n} = \sum_{i=1}^{nl} \lambda^{\beta}_{m,i} \frac{T_n}{T_i} \tag{5-12}$$

where

$\lambda^{c}_{m,n}$	=	burrow collapse rate constant (year-')
$\lambda^{\beta}_{m,i}$	=	soil transport rate constant for compartment i (year-') for burrowing animals
T_n	=	thickness of compartment n (m)
T_i	=	thickness of compartment i (m)
nl	=	the number of compartments lower than compartment i.

5.4.7 Biotic Model Calibration.

The biotic model was not calibrated for two reasons. First, data from surface sampling are inconsistent and probably reflect past operational releases and flooding events rather than biotic uptake. In addition, ongoing recontouring efforts have made data for surface concentrations less useful for calibration purposes. Concentrations of Cs-137 and Co-60 decrease more rapidly than can be accounted for by decay or leaching. Rapid decrease is believed to be caused by the sampling of clean soil used in recontouring. Second, regardless of which potential remedy is selected, it is assumed that some form of recontouring and capping of the waste will be required. Any additional cover would tend to eliminate the potential for biotic intrusion into the waste. With this assumption, effort to calibrate to suspect data did not seem appropriate. If the assumption of additional cover is not appropriate in the future, then additional work on the biotic model would be warranted at that time.

5.4.8 Summary

The DOSTOMAN biotic model was used to predict surface soil concentrations for use in the exposure assessment. The concentrations are believed to be conservative for the processes modeled. However, operational releases and flooding releases were not simulated. The biotic model was not calibrated to measured soil concentrations because (a) soil data were inconsistent for many contaminants, (b) the surface of the SDA is routinely modified by subsidence repair and recontouring, and (c) some form of covering with additional material (i.e., a cap) will be implemented as a component of any remedial action at the SDA. An appropriately designed cover would eliminate the possibility of biotic intrusion into the waste.

5.5 Summary and Conclusions

Modeling presented in this section is the basis for analysis of risk, remedial alternatives, and remedial decisions for OU **7-13/14**. Except for the VOC COPC analysis, modeling in the ABRA is improved compared to the IRA model. Improvements in the inventory and results of characterization activities have been successfully incorporated. Table **5-34** summarizes improvements in the ABRA models compared to the modeling implemented for the IRA. However, results must be considered in the context of uncertainties inherent in the modeling relative to conceptual models and parameterization of the conceptual model that was implemented. For discussion of uncertainties, see Section 6.

Table **5-34**. Summary of improvements in the remedial investigation/feasibility study models compared to the Interim Risk Assessment models.

Topic	IRA Approach	Modifications for the Ancillary Basis for Risk Analysis	Bases for Improvement
Contaminant screening	Assessed 91 radioactive and chemical contaminants (53 quantitatively in 11 groups and 38 qualitatively)	• Simulated fate and transport for contaminants in seven groups. • Only surface pathway risks were assessed for C-137 and Sr-90 (human health) and ecological contaminants of potential concern (COPCs) using DOSTOMAN. • Risk estimates for the three volatile organic compound (VOC) COPCs were scaled from the IRA and not remodeled by Operable Unit (OU) 7-13/14. (Note: OU 7-08 remodeling is planned for calendar year 2003.)	Eliminated contaminants were shown in the IRA to be clearly outside of the cumulative risk ranges for all pathways. Several contaminants with 1E-07 or 0.1 order of magnitude risks or hazard quotients (HQs) were retained based on uncertainties (e.g., Ac-227, Pa-231, Pb-210, with groundwater concentrations still rising at the 10,000-year simulation period; methylene chloride and tetrachloroethylene because of uncertain VOC disposal quantities).
Source term inventory	Contaminant Inventory Database for Risk Assessment (CIDRA) best-estimate inventories through 1993 used for limited calibration, upper-bound inventories used for base case risk estimates, and projected inventories not assessed.	Corrected CIDRA best-estimate inventories were used to generate base-case risk estimates. Uncertainties in inventories were assessed by simulating corrected upper-bound quantities and the projected maximum limits on the facility disposal quantities.	CIDRA revisions: • Projected disposal data replaced with actual disposal quantities for 1994 to 1999 • Adjusted to include estimated historical Idaho National Engineering and Environmental Laboratory (INEEL) reactor operations waste.
Source discretization	Three time periods reflecting the types of disposal operations that were simulated are: 1950 to 1970, 1971 to 1983, and 1983 to 1993	The CIDRA inventories were proportioned into 13 discrete source areas based on shipping information in the WasteOScope database.	Revisions to CIDRA and development of WasteOScope database.

Table **5-34.** (continued)

Topic	IRA Approach	Modifications for the Ancillary Basis for Risk Analysis	Bases for Improvement
C-14 risk	Based on CIDRA upper-bound inventories and release rates from literature reviews of corrosion data	Revised inventory, mobility (K_d), and site-specific corrosion rates were used.	Revised inventory (see above), mobility, and site-specific corrosion test data.
Volatile organic contaminant mass remaining in the waste	• The CIDRA best-estimate inventories were doubled for both model calibration and base-case risk • The VOC mass removed by the ongoing extraction was not accounted for • Conservative diffusion from the sludge was simulated.	Scaled concentrations and risks based on inventory corrections.	Disposal records showed actual number and weight of buried organic sludge.
Uranium risk	Unlimited solubility.	Unlimited solubility.	Addressed solubility limits in uncertainty based on Eh and pH combinations possible in waste.
Interbed hydrologic and transport properties	Used average values estimated from site-specific data where available and literature values in other cases.	Included spatial variability in hydrologic properties in the B-C and C-D interbeds.	• Cores collected in calendar year 2000 were analyzed to profile hydrologic properties • Cores collected in calendar year 2000 were analyzed to improve basis for site-specific uranium and neptunium partition coefficients.
Interbed lithology	Kriged available values.	Used updated kriging with additional information.	New well data (e.g., interbed tops and thicknesses from 22 vadose zone and aquifer wells installed in calendar year 2000).
Infiltration rates	Source term model used spatially averaged value of 8.5 cm/year.	A unique infiltration rate was implemented for each of the 13 source areas.	Model change allowing discrete infiltration rates for each of the areas.
Aquifer boundary conditions	Interpolated from 1994 to 1995 measured water levels.	Additional data were used to update the aquifer model.	Water level measurements from expanded monitoring network.
Upgradient contributions	Upgradient contribution assumed not to occur.	Looked for upgradient contributions but detected no discernable impact.	Ongoing work to help fingerprint isotopes and determine if upgradient impact exists.

Table 5-34. (continued)

Topic	IRA Approach	Modifications for the Ancillary Basis for Risk Analysis	Bases for Improvement
Sporadic low-level detections of actinides in aquifer	Assumed to be anomalous or related to upgradient influences.	Not included.	Isotopic analysis (thermal ionization mass spectrometry) of aquifer samples from across the INEEL delayed so results are not available to support this analysis.
Separation of vadose zone and aquifer simulation domains for dissolved-phase transport	Combined domains to consider downgradient off-gassing.	Separated domains for vadose zone and aquifer.	None necessary, simply a modeling change.
Calibration of vadose zone flow model	Used perched water locations and temporal behavior as targets (poor results).	Updated properties for the B-C and C-D interbeds.	New data from core collected from the 22 wells drilled in 1999 and 2000.
Calibration of aquifer flow model	Steady-state calibration using three values assigned to specific zones in the aquifer and a value developed by Waste Area Group 3 to the I-Basalt at depth.	Steady-state calibration to improved water-level data set and kriged aquifer permeabilities before calibration.	Additional water level data from expanded monitoring network (routinely measured during quarterly sampling).
Partition coefficient assignments	Used data from Dicke (1997), which included site-specific values when available and values from other literature.	Used data from Dicke (1997) except for revised value for **C-14.**	Site-specific 2000 core interbed sample analysis shows the K_d values in Dicke (1997) for uranium and neptunium are on the conservative end of the range. Dicke (1998) provides a site-specific C-14 value of 0.1 mL/g instead of **5** mL/g.
Facilitated transport	Assumed not to occur.	Three sensitivity cases implemented using 1E-02, 1E-04, and 1E-06 fractions of the plutonium mass.	Clemson column studies indicate less than 1% facilitated transport.
Spreading area influences	Assumed not to occur.	Included influence as part of base case and implemented sensitivity runs with no influence and with double the influence modeled in the base case.	1999 U.S. Geological Survey tracer test results and total chemistry sampling to include chlorine to bromine ratios.

In each case, best judgment was used in implementing the source-release model and the subsurface flow and transport model. Lack of data for calibrating the source-release model and the subsurface flow and transport model for strictly dissolved contaminants has resulted in an ongoing monitoring program representing considerable investment of time and expenditure of money. Eventually, results of these monitoring activities will improve the ability to simulate processes occurring in the subsurface.

Currently, results of these models are useful in estimating potential risks to human health and the environment and assessing appropriate remedial alternatives to mitigate unacceptable risk. However, results must be considered in light of uncertainties associated with this analysis. Existing data sets for dissolved-phase contaminants were inadequate for model calibration; therefore, model parameters were not adjusted in an attempt to achieve calibration by improving agreement between simulated and observed results. Comparisons were made to assess model predictions relative to observed results. Several sensitivity cases were completed that indicate the results of the modeling are generally conservative.

Future activities that would improve the overall ability of the **ABRA** model to represent the movement of contaminants in the subsurface include the following:

- Sensitivity of risk results to the infiltration regime through the waste was demonstrated in a sensitivity case. This result points out the importance of continuing the monitoring and interpretation of data being collected by the **SDA** Type **A** and **B** probes. Hydrologic conditions within the waste and leachate contaminant concentrations are particularly important.

- Monitoring data from the deep vadose zone monitoring network should be incorporated to update and improve the subsurface flow and transport model. The model used in the ABRA is inadequately calibrated. ***An*** influence appears to exist in observed aquifer concentrations from dissolved-phase nonsorbing transport of nitrate as well as a potential impact from hexavalent chromium. Monitoring and data interpretation to determine if these constituents are truly useful for model calibration should be continued. Monitoring of the vadose zone network also should be continued to improve the delineation of the extent of lateral influence from the spreading areas within the vadose zone.

- The low-permeability zone within the aquifer has previously been demonstrated to exert a large influence on predicted concentrations and risks. Continued monitoring and interpretation of ongoing tracer testing within the aquifer is necessary to improve understanding the extent of this low-permeability zone. The flat nature of the water table in the **SDA** vicinity has made determining direction of local water flow within the aquifer difficult. **A** proposed method to use existing isobaric wells at the **SDA** to more accurately measure water levels could also improve the state of knowledge regarding directions of groundwater flow.

- Evaluating the likelihood of fast pathways down through the interbeds should be continued. Part of this evaluation should include taking interbed samples for measuring hydrologic and transport properties, if any additional wells are drilled in the **SDA** vicinity. Spatially variable K_ds in the interbeds could not be included based on the currently available data. The data set resulting from the calendar year **1999** drilling campaign represents a good start, but spatial structure in the K_ds could not be identified.

- Another reason to make additional measurements of hydrologic and transport properties on interbed samples is to compare the K_ds used in the **ABRA** for uranium and neptunium to the distribution of measured values in Hull **(2001).** If the basis could be improved by increasing the number of samples on which analyses had been conducted, the assigned K_ds for the interbeds could be justifiably increased, which would result in substantial changes in the time period within which concentration increases in the aquifer are simulated to occur.

- Modeling VOCs should be conducted with the improved ABRA model and should include or use (a) new inventory data, (b) estimates of VOC mass remaining in the pits, (c) information from the recently completed flux chamber and source-release studies, (d) updated mass removal data from operation of the VVE system, (e) updated monitoring data, and (f) all other improvements listed in this section (e.g., spreading area influences and aquifer flow analysis).

5.6 References

Abbott, M. L., L. Fraley Jr., and T. D. Reynolds, 1991, "Root Profiles of Selected Cold Desert Shrubs and Grasses in Disturbed and Undisturbed Soils," ***Environmental & Experimental Botany*** 31, pp. 165-178.

Adler Flitton, M. Kay, Carolyn W. Bishop, Ronald E. Mizia, Lucinda L. Torres, and Robert D. Rogers, 2001, ***Long Term Corrosion/Degradation Test Third-Year Results,*** **INEEL/EXT-01-00036,** Idaho National Engineering and Environmental Laboratory, Bechtel BWXT Idaho, LLC, Idaho Falls, Idaho.

Anderson, J. E., 1991, ***Vegetation Studies to Support the NPR Environmental Impact Statement,*** NPR-DEIS-SR-003, Environmental Science and Research Laboratory, U.S. Department of Energy Idaho Operations Office, Idaho Falls, Idaho.

Anderson, J. E., and R. Inouye, 1988, ***Long-Term Dynamics of Vegetation in Sagebrush Steppe of Southeastern Idaho,*** Final Report, Task Order 5, Modification 21, Contract No. C84130479, Department of Biological Sciences, Idaho State University, Pocatello, Idaho.

Anderson, J. E., R. J. Jeppson, R. J. Rjwilkosz, G. M. Marlette, and K. E. Holte, 1978, "Trends in Vegetation Development on the Idaho National Engineering Laboratory Site," ed. O. D. Markham, ***Ecological Studies on the Idaho National Engineering Laboratory Site 1978 Progress Report,*** IDO-12087, Environmental Science and Research Laboratory, U.S. Department of Energy Idaho Operations Office, Idaho Falls, Idaho.

Anderson, S. R., D. A. Ackerman, M. J. Liszewski, and R. M. Freiburger, 1996, ***Stratigraphic Data for Wells at and near the Idaho National Engineering Laboratory, Idaho,*** DOEAD-22127, U.S. Geological Survey Open-File Report 96-248, U. S. Geological Survey.

Arnett, R. C., and R. P. Smith, 2001, "WAG 10 Groundwater Modeling Strategy and Conceptual Model," INEEL/EXT-01-00768 Rev. B, Idaho National Engineering and Environmental Laboratory, Bechtel BWXT Idaho, LLC, Idaho Falls, Idaho.

Arthur, W. J., and O. D. Markham, 1982, "Ecological Vectors of Radionuclide Transport at a Solid Radioactive Waste Disposal Facility in Southeastern Idaho," ed. M. A. Feraday, ***Proceedings of the International Conference on Radioactive Waste Management, Winnipeg, Manitoba, Canada, September 12–15, 1982,*** ISBN 0-919784-01-1, Canadian Nuclear Society, Toronto, Ontario, Canada.

Arthur, W. J. 111, 1982, "Radionuclide Concentrations in Vegetation at a Solid Radioactive Waste-Disposal Area in Southeastern Idaho," ***Journal of Environmental Quality,*** Vol. 11, No. 3, pp. 394–399.

Baca, Robert G., Swen O. Magnuson, Hoa D. Nguyen, and Pete Martian, 1992, *A Modeling Study of Water Flow in the Vadose Zone Beneath the Radioactive Waste Management Complex,* EGG-GEO-10068, Idaho National Engineering and Environmental Laboratory, EG&G Idaho, Idaho Falls, Idaho.

Becker, B. H., J. D. Burgess, K. J. Holdren, D. K. Jorgensen, S. O. Magnuson, and A. J. Sondrup, 1998, *Interim Risk Assessment and Contaminant Screening for the Waste Area Group 7 Remedial Investigation,* DOE/ID-10569, U.S. Department of Energy Idaho Operations Office, Idaho Falls, Idaho.

Becker, B. H., 1997, *Selection and Development of Models Used in the Waste Area Group 7 Baseline Risk Assessment,* INEL/EXT-97-00391, Idaho National Engineering and Environmental Laboratory, Lockheed Martin Idaho Technologies Company, Idaho Falls, Idaho.

Becker, B. H., T. A. Bensen, C. S. Blackmore, D. E. Burns, B. N. Burton, N. L. Hampton, R. M. Huntley, R. W. Jones, D. K. Jorgensen, S. O. Magnuson, C. Shapiro, and R. L. VanHorn, 1996, *Work Plan for Operable Unit 7-13/14 Waste Area Group 7 Comprehensive Remedial Investigation/Feasibility Study,* INEL-95/0343, Idaho National Engineering and Environmental Laboratory, Lockheed Martin Idaho Technologies Company, Idaho Falls, Idaho.

Becker, B. H, C. A. Loehr, S. M. Rood, and J. A. Sondrup, 1994, *Risk Assessment of Remedial Objectives for Nontransuranic Waste in Pit 9,* EGG-ER-11093, Rev. 1, Idaho National Engineering and Environmental Laboratory, EG&G Idaho, Idaho Falls, Idaho.

Blom, P. E., W. H. Clark, and J. B. Johnson, 1991, "Colony Densities of the Seed Harvesting Ant *Pogonomyrmex salinus* (Hymenoptera: Formicidae) in Seven Plant Communities on the Idaho National Engineering Laboratory," *Journal of the Idaho Academy of Science,* Vol. 27, No. 1, pp. 28-36.

Blom, P. E., J. B. Johnson, and S. K. Rope, 1991, "Concentrations of ^{137}Cs and ^{60}Co in Nests of the Harvester Ant, Pogonomyrex Salinus, and Associated Soils near Nuclear Reactor Waste Water Ponds," *American Midland Naturalist,* Vol. 126, pp. 140-151.

Boone, J. D., 1990, *Ecological Characteristics and Preferential Edge Use of Small Mammal Populations Inhabiting a Radioactive Waste Disposal Area,* M.S. Thesis: Idaho State University, Pocatello, Idaho.

Boone, J. D., and B. L. Keller, 1993, "Temporal and Spatial Patterns of Small Mammal Density and Species Composition on a Radioactive Waste Disposal Area: the Role of Edge Habitat," *Great Basin Naturalist,* Vol. 53, No. 4, pp. 341-349.

Brooks, R. H., and A. T. Corey, 1966, "Properties of Porous Media Affecting Fluid Flow," *J. Irrig. Drain. Div.,* American Society of Civil Engineering, Vol. 92 (IR2), pp. 61-88.

Burgess, J. D., 1996, *Tritium and Nitrate Concentrations at the RWMC,* Engineering Design File EDF-ER-024, INEL-961204, Idaho National Engineering and Environmental Laboratory, Lockheed Martin Idaho Technologies Company, Idaho Falls, Idaho.

Case, Marilyn J., Arthur S. Rood, James M. McCarthy, Swen O. Magnuson, Bruce H. Becker, and Thomas K. Honeycutt, 2000, *Technical Revision of the Radioactive Waste Management Complex Low-Level Waste Radiological Performance Assessment for Calendar Year 2000,* INEEL/EXT-2000-01089, Idaho National Engineering and Environmental Laboratory, Bechtel BWXT Idaho, LLC, Idaho Falls, Idaho.

Cecil, L. D., J. R. Pittman, T. M. Beasley, R. L. Michel, P. W. Kubik, P. Sharma, U. Fehn, and H. Gove, 1992, "Water Infiltration Rates in the Unsaturated Zone at the Idaho National Engineering Laboratory Estimated from Chlorine-36 and Tritium Profiles, and Neutron Logging," *Proceedings of the 7th International Symposium on Water-Rock Interaction*, WRI-7, Park City, Utah.

Cline, J. F., F. G. Burton, D. A. Cataldo, W. E. Skiens, and K. A. Gano, 1982, *Long-Term Biobarriers to Plant and Animal Intrusion of Uranium Tailings*, DOE/UMT-0209, Pacific Northwest Laboratory, Richland, Washington.

Dicke, C. A., 1998, *Carbon-I4 Distribution Coeficients Measured from Batch Experiments on SDA Sediments*, INEEL/INT-98-00068, Engineering Design File EDF-RWMC-1011, Idaho National Engineering and Environmental Laboratory, Lockheed Martin Idaho Technologies Company, Idaho Falls, Idaho.

Dicke, C. A., 1997, *Distribution Coeficients and Contaminant Solubilities for the Waste Area Group 7 Baseline Risk Assessment*, INEL/EXT-97-00201, Idaho National Engineering and Environmental Laboratory, Lockheed Martin Idaho Technologies Company, Idaho Falls, Idaho.

DOE-ID, 1998, *Addendum to the Work Plan for the Operable Unit 7-13/14 Waste Area Group 7 Comprehensive Remedial InvestigatiodFeasibility Study*, DOE/ID-10622, *U.S.* Department of Energy Idaho Operations Office, Idaho Falls, Idaho.

DOE-ID, 1994, *Track* 2 *Sites: Guidance for Assessing Low Probability Hazard Sites at the INEL*, DOE/ID-10389, Rev. 6, U.S. Department of Energy Idaho Operations Office, Idaho Falls, Idaho.

EPA, 1999, *Understanding Variation in Partition Coeficient, K_d Values*, EPA 402-R—99-004A&B, Office of Radiation and Indoor Air, U. S. Environmental Protection Agency.

Fabryka-Martin, J., A. Flint, G. Gee, "Peer Review Team Report on Conceptual Models and Field Verification of Radionuclide Transport through the Vadose Zone at INEEL," Final Report, November 5, 1998, prepared for Idaho National Engineering and Environmental Laboratory.

Fitzner R. E., K. A. Gano, W. H. Rickard, and L. E. Rogers, 1979, *Characterization of the Hanford 300 Area Burial Grounds, Task IV-Biological Transport*, PNL-6779, Pacific Northwest Laboratory, Hanford, Washington.

Freeze, R. A., and J. A. Cherry, 1979, *Groundwater*, Englewood Cliffs, New Jersey: Prentice-Hall.

Gaglio, M. D., W. P. Mackay, E. A. Osorio, and I. Iniguez, 1998, "Nest Populations of *Pogonomyrmex salinus* Harvester Ants (Hymenoptera: Formicidae)," *Sociobiology*, Vol. 332, pp. 459-463.

GE, 1989, *Nuclides and Isotopes Fourteenth Edition Chart of the Nuclides*, General Electric Nuclear Energy.

Gelhar, L. W., 1986, "Water Resources Research," Volume 22, No. 9, August 1986 Supplement, pp. 135S-145S.

Glover, P. A., F. J. Miner, and W. O. Polzer, 1976, "Plutonium and Americium Behavior in the Soil/Water Environment, I., 'Sorption of Plutonium and Americium by Soils,"' *Proceedings of Actinide-Sediment Reactions Working Meeting, Seattle, Washington,* BNWL-2117, pp. 225-254, Battelle Pacific Northwest Laboratories, Richland, Washington.

Grossman, Christopher J., Robert A. Fjeld, John T. Coates, and Alan W. Elzerman, 2001, *The Sorption of Selected Radionuclides in Sedimentary Interbed Soils from the Snake River Plain,* INEEL/EXT-01-01106, Clemson University, Clemson, South Carolina, Idaho National Engineering and Environmental Laboratory, Bechtel BWXT Idaho, LLC, Idaho Falls, Idaho.

Groves, C. R., and B. Keller, 1983, "Ecological Characteristics of Small Mammals on a Radioactive Waste Disposal Area in Southeast Idaho," *American Midland Naturalist,* Vol. 109, *No.* 2.

Groves, C. R., 1981, *The Ecology of Small Mammals on the Subsurface Disposal Area, Idaho National Engineering Laboratory Site,* M.S. Thesis: Idaho State University, Pocatello, Idaho.

Hackett, W. R., J. A. Tullis, R. P. Smith, S. J. Miller, T. V. Dechert, P. A. McDaniel, and A. L. Falen, 1995, *Geologic Processes in the RWMC Area, Idaho National Engineering Laboratory: Implications for Long Term Stability and Soil Erosion at the Radioactive Waste Management Complex,* INEL-95/0519, Idaho National Engineering and Environmental Laboratory, Lockheed Martin Idaho Technologies Company, Idaho Falls, Idaho.

Hampton, N. L., 2001, *Biological Data to Support Operable Unit 7-13/14 Modeling of Plant and Animal Intrusion at Buried Waste Sites,* INEEL/EXT-01-00273, Rev.0, Idaho National Engineering and Environmental Laboratory, Bechtel BWXT Idaho, LLC, Idaho Falls, Idaho.

Hampton, N. L., and T. A. Benson, 1995, *SDA Biotic Data Compilation,* Engineering Design File EDF-ER WAG7-76, INEL-951139, Idaho National Engineering and Environmental Laboratory, Lockheed Martin Idaho Technologies Company, Idaho Falls, Idaho.

Hull, A. C., Jr., and G. J. Klomp, 1974, "Yield of Crested Wheatgrass Under Four Densities of Big Sagebrush in Southern Idaho," *Technical Bulletin* No. *1483,* Agricultural Research Service, U.S. Department of Agriculture.

Hull, Larry, 2001, Interoffice Memorandum to Theodore J. Meyer, Doug Bums, Swen Magnuson, and James McCarthy, "Approach to Simulation of Actinides for the OU 7-13/14 Baseline Risk Assessment," Idaho National Engineering and Environmental Laboratory, Bechtel BWXT Idaho, LLC, Idaho Falls, Idaho, LCH-04-01, April 4, 2001.

INEEL, 2002a, *User's Manual for the WasteOScope Operable Unit 7-13/14 Mapping Software,* INEEL/EXT-01-01585, Rev. 0., Idaho National Engineering Laboratory, Bechtel BWXT Idaho, LLC, Idaho Falls, Idaho, March 2002.

INEEL, 2002b, *Waste Area Group 7 Geographic Information Systems WasteOScope Application,* INEEL/EXT-02-00292, Rev. 0., Idaho National Engineering and Environmental Laboratory, Bechtel BWXT Idaho, LLC, Idaho Falls, Idaho, March 2002.

Klepper, E. L., K. A. Gano, L. L. Cadwell, 1985, *Rooting Depth and Distributions of Deep-Rooted Plants in the 200 Area Control Zone of the Hanford Site,* PNL-5247, Pacific Northwest Laboratory, Battelle Memorial Institute, Hanford, Washington.

Klepper, E.L., L. E. Rogers, J. D. Hedlund, and R. G. Schreckhise, 1979, *Radioactivity Associated with Biota and Soil of the 216-A-24 Crib*, PNL-1948, Pacific Northwest Laboratory, Hanford, Washington.

Knobel, L. L., B. R., Orr, and L. D. Cecil, 1992, "Summary of Background Concentrations of Selected Radiochemical and Chemical Constituents in Groundwater from the Snake River Plain Aquifer, Idaho: Estimated from an Analysis of Previously Published Data," *Journal of the Idaho Academy of Science*, Vol. *28*, X10.1, p. 48.

Koehler, D. K., 1988, *Small Mammal Movement Patterns Around a Radioactive Waste Disposal Area in Southeastern Idaho*, M.S. Thesis: University of Wyoming, Laramie, Wyoming.

Kudera, D. E., and B. W. Brown, 1996, *Volatile Organic Compounds Disposed of from 1952 Through 1983 at the Radioactive Waste Management Complex: Quantities Forms, Release Mechanisms and Rates*, ER-WAG7-90, Idaho National Engineering and Environmental Laboratory, Lockheed Martin Idaho Technologies Company, Idaho Falls, Idaho.

Landeen, D. S., and R. M. Mitchell, 1981, "Invasion of Radioactive Waste Burial Sites by the Great Basin Pocket Mouse *(Perognathus parvus)*," *International Symposium on Migration in the Terrestrial Environment of Long-lived Radionuclides from the Nuclear Fuel Cycle, Knoxville, Tennessee, July 27-31*, RHO-SA-211.

Laundre, J. W., 1989a, "Horizontal and Vertical Diameter of Burrows of Five Small Mammal Species in Southeastern Idaho," *Great Basin Naturalist*, 1989, Vol. 49, pp. 646–649.

Laundre, J. W., 1989b, "Burrows of Least Chipmunks in Southeastern Idaho," *Northwestern Naturalist*, Vol. 70, pp. 18–20.

Leecaster, Molly K., 2002, *Geostatistic Modeling of Subsurface Characteristics in the Radioactive Waste Management Complex Region, Operable Unit 7-13/14*, INEEL/EXT-02-00029, Rev. *0*. Idaho National Engineering and Environmental Laboratory, Idaho Falls, Idaho, Bechtel BWXT Idaho, LLC, Idaho Falls, Idaho.

Lerman, A., 1988, "*Geochemical Processes Water and Sediment Environments,*" Reprint ed., Melbourne, Florida: Krieger Publishing Company.

Lindzey, F. G., 1976, "Characteristics of the Natal Den of the Badger," *Northwest Science*, Vol. *50*, No. 3, pp. 178–180.

LMITCO, 1995, ***A** Comprehensive Inventory of Radiological and Nonradiological Contaminants in Waste Buried in the Subsurface Disposal Area of the INEL RWMC During the Years 1952–1983*, INEL-95/03 10 (formerly EGG-WM-10903), Rev. 1, Idaho National Engineering and Environmental Laboratory, Lockheed Martin Idaho Technologies Company, Idaho Falls, Idaho.

Magnuson, S. O., and A. J. Sondrup, 1998, *Development, Calibration, and Predictive Results of a Simulator for Subsurface Pathway Fate and Transport of Aqueous- and Gaseous-Phase Contaminants in the Subsurface Disposal Area at the Idaho National Engineering and Environmental Laboratory*, INEEL/EXT-097-00609, Idaho National Engineering and Environmental Laboratory, Lockheed Martin Idaho Technologies Company, Idaho Falls, Idaho.

Magnuson, S. O., 1995, *Inverse Modeling for Field-Scale Hydrologic and Transport Parameters of Fractured Basalt*, INEL-95/0637, Idaho National Engineering and Environmental Laboratory, Lockheed Martin Idaho Technologies Company, Idaho Falls, Idaho.

Magnuson, S. O. and D. L. McElroy, 1993, *Estimation of Infiltration from In Situ Moisture Contents and Representative Moisture Characteristic Curves for the 30-, 110-, and 240-ft Interbeds*, Engineering Design File RWM-93-001.1, EG&G Idaho, Idaho Falls, Idaho.

Maheras, S. J., A. S. Rood, S. O. Magnuson, M. E. Sussman, and R. N. Bhatt, 1994, *Radioactive Waste Management Complex Low-Level Waste Radiological Performance Assessment*, EGG-WM-8773, Idaho National Engineering and Environmental Laboratory, EG&G Idaho, Idaho Falls, Idaho.

Martian, P., 1995, *UNSAT-H Infiltration Model Calibration at the Subsurface Disposal Area, Idaho National Engineering Laboratory*, INEL-990596, Idaho National Engineering and Environmental Laboratory, Lockheed Martin Idaho Technologies Company, Idaho Falls, Idaho.

MathSoft, 2000, *S+SPATIALSTATS User's Manual Version 1.5*, Data Analysis Products Division, Mathsoft, Seattle, Washington.

McCarthy, J. M., B. H. Becker, S. O. Magnuson, K. N. Keck, and T. K. Honeycutt, 2000, *Radioactive Waste Management Complex Low-Level Waste Radiological Composite Analysis*, INEEL/EXT-97-01113, Idaho National Engineering and Environmental Laboratory, Bechtel BWXT Idaho, LLC, Idaho Falls, Idaho.

McCarthy, J. M., R. C. Arnett, R. M. Neupauer, M. J. Rohe, and C. Smith, 1995, *Development of a Regional Groundwater Flow Model for the Area of the Idaho National Engineering Laboratory, Eastern Snake River Plain Aquifer*, INEL-95/0169, Rev. 1, Idaho National Engineering and Environmental Laboratory, Lockheed Martin Idaho Technologies Company, Idaho Falls, Idaho.

McKenzie, D. H., L. L. Caldwell, C. E. Cushing Jr., R. Harty, W. E. Kennedy Jr., M. A. Simmons, J. K. Soldat, and B. Swartzman, 1982, *Relevance of Biotic Pathways to the Long-Term Regulation of Nuclear Waste Disposal*, NUREG/CR-2675, U.S. Nuclear Regulatory Commission.

Merck, 1989, *An Encyclopedia of Chemicals, Drugs, and Biologicals*, 11th ed., Rahway, New Jersey: Merck & Co. Publishing.

Miller, Eric C., and Mark D. Varvel, 2001, *Reconstructing Past Disposal of 743 Series Waste in the Subsurface Disposal Area for Operable Unit 7-08, Organic Contamination in the Vadose Zone*, INEEL/EXT-01-00034, Rev. 0, Idaho National Engineering and Environmental Laboratory, Bechtel BWXT Idaho, LLC, Idaho Falls, Idaho.

Miller, E. C., and J. D. Navratil, 1998, *Estimate of Carbon Tetrachloride in 743 Series Sludges Buried in the Subsurface Disposal Area at the Radioactive Waste Management Complex*, INEEL/EXT-98-00112, Rev. 0, Idaho National Engineering and Environmental Laboratory, Lockheed Martin Idaho Technologies Company, Idaho Falls, Idaho.

Miner, F. J., P. A. Evans, and W. L. Polzer, 1982, "Plutonium Behavior in the Soil/Water Environment Part I. Sorption of Plutonium by Soils," RFP-2480, Rocky Flats Plant, Golden, Colorado.

Nagata, P. K., and J. Banaee, 1996, ***Estimation of the Underground Corrosion Rates for Low-Carbon Steels: Types 304 and 316 Stainless Steels; and Inconel 600, 601, and 718 Alloys at the Radioactive Waste Management Complex,*** INEL096/098, Idaho National Engineering and Environmental Laboratory, Lockheed Martin Idaho Technologies Company, Idaho Falls, Idaho.

Newman, M. E., and F. M. Dunnivant, 1995, ***Results from the Large-Scale Infiltration Test: Transport of Radionuclide Tracers,*** Engineering Design File EDF-ER-WAG7-77, INEL-951146, Idaho National Engineering and Environmental Laboratory, Lockheed Martin Idaho Technologies Company, Idaho Falls, Idaho.

Nimmo, J. R., K. S. Perkins, P. A. Rose, J. P. Rousseau, B. R. Orr, B. V. Twining, and S. R. Anderson, 2002, "Rapid Transport of Naphthalene Sulfonate Tracer in the Unsaturated and Saturated Zones near the Big Lost River Flood-Control Areas at the Idaho National Engineering and Environmental Laboratory," Submitted to the ***Vadose Zone Journal.***

NRCS, 1981, ***NRCS Range Site Descriptions for MLRA,*** BLM-BLMB-B1lb, National Resource Conservation Service.

Orr, B. R., L. D. Cecil, and L. L. Knobel, 1991, ***Background Concentrations of Selected Radionuclides, Organic Compounds, and Chemical Constituents in Ground Water in the Vicinity of the Idaho National Engineering Laboratory,*** DOE/ID-22094, U.S. Department of Energy, Idaho Operations Office, Idaho Falls, Idaho.

Oztunali, O. I., and G. W. Roles, 1985, ***Update of Part 61 Impacts Analysis Methodology,*** NUREG/CR-4370, Vol. 1, U.S. Nuclear Regulatory Commission.

Pearson, L. C., 1965, "Primary Production in Grazed and Ungrazed Desert Communities of Eastern Idaho," ***Ecology***, Vol. 46, pp. 278–285.

Reynolds, T. D., and L. L. Fraley Jr., 1989, "Root Profiles of Some Native and Exotic Plant Species in Southeastern Idaho," ***Environmental and Experimental Botany,*** Vol. 29, No. 2. pp. 241–248.

Reynolds, T. D., 1990, "Root Mass and Vertical Root Distribution of Five Semi-Arid Plant Species," ***Health Physics,*** Vol. 58, No. 2.

Reynolds, T. D., and J. W. Laundre, 1988, "Vertical Distribution of Soil Removed by Four Species of Burrowing Rodents in Disturbed and Undisturbed Soils," ***Health Physics,*** 1988, Vol. 54, No. 4, pp. 445-450.

Reynolds, T. D., and W. L. Wakkinen, 1987, "Characteristics of the Burrows of Four Species of Rodents in Undisturbed Soils in Southeastern Idaho," ***American Midland Naturalist,*** Vol. 118, No. 2, pp. 245–250.

Roback, R. C., T. M. Johnson, T. L. McLing, M. T. Murrell, S. Luo, and T. L. Ku, 2001, "Uranium isotopic evidence for groundwater chemical evolution and flow patterns in the eastern Snake River Plain aquifer, Idaho," ***Geological Society of America Bulletin,*** Vol. 113, pp. 1133-1141.

Robertson, J. B., 1974, ***Digital Modeling of Radioactive and Chemical Waste Transport in the Snake River Plain Aquifer at the National Reactor Testing Station, Idaho,*** IDO-22054, U.S. Geological Survey Open File Report, U.S. Geological Survey.

Robertson, J. B., R. Schoen, J. T. Barraclough, 1974, "The Influence of Liquid Waste Disposal on the Geochemistry of Water at the National Reactor Testing Station, Idaho: 1952-1970, IDO-22053," U.S. Geological Survey Open File Report, U.S. Geological Survey.

Rodriguez, R. R., A. L. Schafer, J. McCarthy, P. Martian, D. E. Burns, D. E. Raunig, N. A. Burch, and R. L. Van Horn, 1997, *Comprehensive RI/FS for the Idaho Chemical Processing Plant OU 3-13 at the INEEL—Part A. RI/BRA Report (Final)*, DOE/ID-10534, U. S. Department of Energy Idaho Operations Office, Idaho Falls, Idaho.

Rood, A. S., 1999, *GWSCREEN: A Semi-Analytical Model for Assessment of the Groundwater Pathway from Surface or Buried Contamination, Theory and User's Manual Version 2.5,* INEELEXT-9800750, Idaho National Engineering and Environmental Laboratory, Lockheed Martin Idaho Technology Company, Idaho Falls, Idaho.

Root, R. W. Jr., 1981, *Documentation and User's Guide for "DOSTOMAN," A Pathways Computer Modelf Radionuclide Movement*, DPST-81-549, Idaho National Engineering and Environmental Laboratory, EG&G Idaho, Idaho Falls, Idaho.

Shleien, B., ed., 1992, *The Health Physics and Radiological Health Handbook*, revised ed., Scinta, Silver Spring, Maryland.

Shuman, R. D., M. J. Case, and S. K. Rope, 1985, *Documentation of a Simple Environmental Pathways Model of the Radioactive Waste Management Complex at the Idaho National Engineering Laboratory*, EGG-WM-6916, Idaho National Engineering and Environmental Laboratory, EG&G Idaho, Idaho Falls, Idaho.

Sondrup, A. J., 1998, *Preliminary Modeling of VOC Transport for Operable Unit 7-08, Evaluation of Increased Carbon Tetrachloride Inventory*, INEEL/EXT-2000-00849, Rev. *0*, Idaho National Engineering and Environmental Laboratory, Bechtel BWXT Idaho, LLC, Idaho Falls, Idaho.

Sullivan, T. M., 1993, *DUST Data Input Guide*, NUREG/CR-6041, U.S. Nuclear Regulatory Commission.

Sullivan, T. M., 1992, *Development of DUST: A Computer Code That Calculates Release Rates from LLW Disposal Unit*, BNL-NUREG-47118, Brookhaven National Laboratory, U.S. Nuclear Regulatory Commission.

USGS, 2001, "Science for a Changing World," **http://water.usgs.gov/id/nwis**, April 17, 2001.

USGS, 1998, "Significant Issues to Be Resolved to Support and Defend the Interim Risk Assessment and Additional Work Required to Resolve Those Issues," Letter report from J. P. Rousseau to K. E. Hain, U.S. Department of Energy, Idaho Operations Office, U.S. Geological Survey, Idaho Falls, Idaho.

van Genuchten, M. T., 1980, "A closed-Form Equation for Predicting the Hydraulic Conductivity of Unsaturated Soils," Solo *Science Society of America Journal*, Vol. 44, pp. 892-898.

Varvel, Mark D., 2001, *Mass Estimates of Organic Compounds Buried in the Subsurface Disposal Area for Operable Unit 7-08 and 7-13/14*, INEEL/EXT-01-00277, Engineering Design File EDF-ER-301, Rev. 0, Idaho National Engineering and Environmental Laboratory, Bechtel BWXT Idaho, LLC, Idaho Falls, Idaho.

Vigil, M. J., 1988, *Initial Estimate of Hazardous Waste Constituents in Pit 9*, Engineering Design File EDF-BWP-02, Idaho National Engineering and Environmental Laboratory, EG&G Idaho, Idaho Falls, Idaho.

Vinsome, P. K. W., and G. M. Shook, 1993, "Multi-Purpose Simulation," *Journal of Petroleum Science and Engineering*, Vol. 9, pp. 29-38.

Visual Numerics, 1996, PV-WAVE Version 6.0 User's Guide, Visual Numerics, Inc., 6230 Lookout Road, Boulder, Colorado.

Whitmire, D. L., 2001, *Summary Report: Simulation of Groundwater Flow near the Subsurface Disposal Area at the Idaho National Engineering and Environmental Laboratory*, INEEL/EXT-01-01643, Rev. 0, North Wind Environmental, Idaho National Engineering and Environmental Laboratory, Bechtel BWXT Idaho, LLC, Idaho Falls, Idaho.

Wilde, D. B., 1978, "A population Analysis of the Pygmy Rabbit (*Sylvilagus idahoensis*) on the INEL Site," Ph.D. Dissertation, Idaho State University, Pocatello, Idaho.

Winsor, T. F., and **F.** W. Whicker, 1980, "Pocket Gophers and Redistribution of Plutonium in Soil," *Health Physics*, Vol. 39, pp. 257–262.

Wood, T. R., 1989, Preliminary Assessment of the Hydrogeology at the Radioactive Waste Management Complex, Idaho National Engineering Laboratory, EGG-WM-8694, Idaho National Engineering and Environmental Laboratory, EG&G Idaho, Idaho Falls, Idaho.